12-2017

Peptoid-modified Bicelles as Surrogate Cell Membranes for Membrane Protein Sensors and Analytics

Helya Najafi
University of Arkansas, Fayetteville

Peptoid-modified Bicelles as Surrogate Cell Membranes for Membrane Protein Sensors and Analytics

A dissertation submitted in partial fulfillment
of the requirements for the degree of
Doctor of Philosophy in Engineering

by

Helya Najafi
Shiraz University
Bachelor of Science in Chemical Engineering, 2007
Sharif University of Technology
Master of Science in Chemical Engineering, 2011

December 2017
University of Arkansas

This dissertation is approved for recommendation to the Graduate Council.

_____
Dr. Shannon Servoss
Thesis Director

_____
Dr. Robert Beitle
Committee Member

_____
Dr. Jerry A. Havens
Committee Member

_____
Dr. Christa Hestekin
Committee Member

_____
Dr. Roger E. Koeppe II
Committee Member

Abstract

Membrane-affiliated interactions are significant in understanding cell function, detecting biomarkers to diagnose disease, and in testing the efficiency of new therapeutic targets. Model membrane systems have been developed to study membrane proteins, allowing for stable protein structure and maintaining native activity. Bicelles, disc-shaped lipid bilayers created by combining long- and short-chain phospholipids, are the model membrane system of focus in this study. Bicelles are accessible from both sides and have a wide size range, which make them attractive for studying membrane proteins without affecting function. In this work, bicelles were functionalized with two peptoids to alter the edge and face chemistry. Peptoids are suitable for this application because of the large diversity of available side chain chemistries that can be easily incorporated in a sequence-specific manner. The peptoids sequence consist of three functional regions to promote insertion into the edge of bicelles. The insertion sequence at the C-terminus contains two alkyl chains and two hydrophobic, chiral aromatic groups that anchor into the bicelle edge or face. The facially amphipathic helix contains chiral aromatic groups on one side that interact with the lipid tails and positively charged groups on the other side, which interact with the lipid head groups. Thiol groups are included at the N-terminus to allow for determination of peptoid location in the bicelle. Bicelle morphology and size were assessed by transmission electron microscopy (TEM) and dynamic light scattering (DLS). Peptoid location in the bicelle was determined by attachment of gold nanoparticles, which confirm preferential incorporation of the peptoid into the bicelle edge or face. Results from this study show that peptoid-functionalized bicelles are a promising model membrane system. Specifically, the designed peptoids sequence were found to incorporate preferentially into the edges and faces of bicelles with 82% and 92% specificity, respectively. Additionally, the peptoid-functionalized bicelles are of similar size and morphology to non-functionalized bicelles. Potential applications

would include customization to anchor in biosensors or facilitate interactions with specific membrane proteins or complexes.

Acknowledgments

I would like to thank Dr. Mourad Benamara and Dr. Betty Martin for valuable TEM training. I would like to thank Dr. Ranil Wickramasinghe for use of and consultation regarding DLS, Dr. Suresh Kumar for use of and consultation regarding CD. I want to acknowledge Arkansas Statewide Mass Spectrometry Facility, and the Arkansas Nano & Bio Materials Characterization Facility for use of equipment.

I would like to thank my advisor, Dr. Shannon Servoss for her continuous support, patience, and encouragement throughout my Ph.D study. I could not have imagined having a better advisor and mentor. She taught me how to become a researcher and she never failed to spare me time, attention and comments I needed on the quality of this work.

I would like to thank my friend Neda Mahmoudi who always supported me and helped me wholeheartedly in my personal and academic life. I would like to thank current and former members of our lab specially Dr. Tammy Rechtin, Dr. Philip Turner, Dr. German Perez-Bakovic, and Jesse Roberts for their guidance and help. I would like to give special thanks to my dissertation committee for giving me valuable input through my PhD studies.

Finally, I would like to thank my family for their constant support. I owe thanks to very special person, my mother, for her continued and unfailing love, support and understanding during my studies. Also I should thank my siblings who give me positive energy and confidence in my life.

Dedications

This dissertation titled *Peptoid-modified Bicelles as Surrogate Cell Membranes for Membrane Protein Sensors and Analytics* is dedicated to my mother and my sister Soheila.

Table of Contents

Chapter 1 Introduction

1.1.Cell Membrane

The basic function of biological membranes is to draw a boundary between or within cells and organelles (Figure 1.1) [1]. This function enables the isolation of different cellular processes during tightly regulated transportation into and across membranes. In addition, many different physiological events like signaling, fusion, and fission occur in membranes. Having a complex composition and dynamic nature, membranes can be connected with each other or isolated spatially and temporally [2-4].

The current view of biological membrane is inspired by the “fluid mosaic” model, first introduced in 1972 by Singer and Nicolson [5]. In this model, which is still reliable after more than forty years, the cell membrane was described as a two-dimensional fluid lipid bilayer where proteins have an asymmetric distribution among the lipids. Recent experimental data showed some facts about biological membrane that are not considered in the fluid mosaic model, such as membrane curvature, high density of transmembrane proteins, and deviations from equilibrium

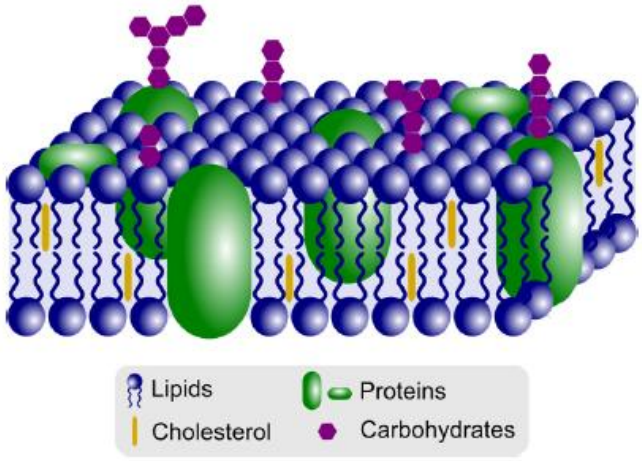

Figure 1.1. Schematic representation of biological membranes [1]

[6]. The lipids are distributed in a bilayer form according to the “fluid mosaic” model, which is in equilibrium. However, experimental data showed that small part of cell membrane may adopt a non-bilayer form. The cell membrane is mainly composed of lipids (50%), proteins (40%), sugars (2%–10%), small amounts of water, inorganic salts, and metal ions.

Investigating the nature of these interconnected components and their reciprocal relationships is very challenging, specifically when scientists try to reestablish membrane biology in the systems which are constructing membranes. Complexity of biological membrane inspire the creation of a vast number of modified, but similar, model systems with precise size, geometry and composition. Generally, cell membrane models have various types from vesicles to different kinds of lipid bilayers [4, 7-9].

1.2.Membrane Protein

Proteins, which have various structures and functions, are the basic building blocks of all living organisms. One class of proteins are membrane proteins, which interact with biological membranes and exist in one-third of the majority of mammalian genomes. They work as ion and molecule transporters and as a selective filter to regulate molecules entering cells. Other functions of membrane proteins include immune system molecule recognition, energy transduction, and communicate with the surrounding environment [10, 11].

Despite membrane protein lesser number in comparison with other soluble counterparts, their importance cannot be overlooked. For instance, they represent 50% of all known drug targets. The function of membrane proteins is to delineate proteins that interact with the plasma membrane of cells. It should be pointed out that not all membrane proteins have similar

interactions with the lipid bilayer of the plasma membrane. Membrane proteins are classified into three groups: peripheral, integral, and lipid-anchored. The interaction between peripheral membrane proteins and plasma membrane of cells is superficially. The common method to extract these kind of proteins is based on traditional biochemical techniques where typically dissolve in aqueous buffers. Integral membrane proteins, which are embedded in the lipid bilayer of the plasma membrane. The degree of association between integral membrane proteins and lipids is variable [7]. Lipid-anchored proteins can dissolve in aqueous buffers and anchor to plasma membrane via the covenant attachment of a glucolipid and a lipid.

Membrane proteins are considered a challenging class of biomolecules to study. This is result due to the high fractions of non-polar amino acids in their structure, which create a high degree of hydrophobicity. Traditional biochemical techniques such as analytical ultracentrifugation, solution NMR, and chromatography have been adapted to study membrane proteins. However, these adapted methods need to be modified experimentally in order to study a new membrane protein. These challenges have encouraged researchers to develop simpler model membrane systems for studying membrane proteins [4].

1.3.Model Cell Membrane

In general, the differences between membrane proteins are subtle. For instance, integral membrane proteins are embedded in the lipid bilayers as a single α-helix, a bundle of α-helices, or β-barrels. Due to the small variations in membrane protein architecture responsible for a specific function, exceptional model membrane systems need to be developed. Moreover, several membrane protein characteristics depend on the membrane environment such as secondary structures, aggregation, dynamics, stability, orientation, and function.

The most commonly used systems for studying membrane proteins are: (1) vesicles, (2) supported lipid bilayers, (3) nanodiscs, and (4) bicelles. Each of these systems has advantages and disadvantages for the study of membrane proteins, which will be further discussed.

1.3.1. Vesicles

Vesicles (lipid vesicles or liposomes) are composed of phospholipid molecules that form bilayers in an aqueous environment because of their amphipathic nature. Vesicles are a lipid bilayer membrane that have an aqueous cavity inside (Figure 2) and have a wide range of applications including in biology, biochemistry and biophysics [12]. Vesicles were first synthesized in the late 1960s [13, 14], and have become very popular in lipid and membrane studies due to the similarity to living cells. Vesicles are typically formed from a lipid solution in a volatile organic solvent. Slow evaporation of the organic solvent creates a thin lipid film on the inside of a glass flask. Vesicles are formed by the hydration of the lipid film [15]. In addition, different methods have been developed for macroscale production of vesicles including electroformation [16], freeze-drying [17], and budding [18].

Vesicles are categorized based on the size and number of lipid bilayers which is called lamellarity. Vesicles composed of one lipid bilayer are unilamellar vesicles, while multilamellar lipid vesicles have several lipid bilayers [19]. Unilamellar vesicles are divided in three categories based on the size which are small unilamellar vesicles (less than 100 nm), large unilamellar vesicles (100-1000 nm) and giant unilamellar vesicles (larger than 1 micron) [1, 19].

A common use of vesicles to in determine lipid phase behavior in aqueous dispersion. In membrane protein studies, they can be useful in examining the phase behavior of binary and ternary lipid mixtures in bilayers. Single liquid phase, two coexisting liquid phases, solid–liquid phase are physical states that are displayed by vesicles depending on the lipid composition. The protein reconstitution can be established on the vesicles easily. The main disadvantage of this system is low thermodynamic stability. Additionally, lipid molecules in the vesicle bilayer are not in flux with the counterpart, since vesicles are not equilibrium systems. This characteristic is a disadvantage of using vesicles in protein membrane studies, because incorporated proteins are not free to interact with each other [7, 20, 21].

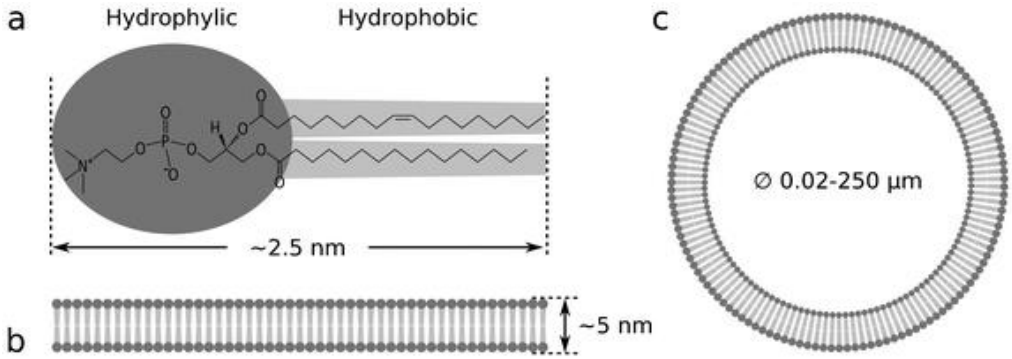

Figure 1.2. (a) The structure of one naturally-occurring lipid molecule, (b) The interaction of the heads and tails of the lipid to self-assemble into a vesicle, and (c) a lipid vesicle [12]

Phospholipid vesicles containing membrane proteins are called proteoliposomes. They should have several characteristics to be considered useful in membrane protein structure and function studies including homogeneous size distribution, uniform distribution of membrane protein in liposomes, high biological activity of embedded membrane protein, and efficiency of protein reconstitution over a variety of lipid to protein ratio [22, 23].

1.3.2. Supported Lipid Bilayers

Supported lipid bilayers (SLB) are flat membranes that are created on a solid substrate and are usually formed by lipid vesicle fusion or Langmuir-Blodgett technique. SLB were introduced in the mid-1980s [24], and often have a very thin (10-20 Å) aqueous layer between the support and the membrane (Figure 1.3A). The solid surface should be hydrophobic, smooth, and clean to form an effective SLB. Common substrates includes fused silica, borosilicate glass, mica, and oxidized silicon [25-27].

The combination of van der Waals, electrostatic, hydration and steric forces keeps the phospholipid membranes above the solid oxide support [28]. Furthermore, it was shown that the aqueous layer between a glass substrate and an egg phosphatidylcholine bilayer is responsible for free movement of lipids with a diffusion constant of 1–4 μm2/s [29]. Recently, air-stable lipid membranes have been introduced as a new class of solid supported lipid bilayers where the bilayer and supporting substrate are separated by an air–water interface [30]. This type of SLB has some limitations. They cannot be used in developing practical biosensors since the membrane needs permanent hydration. Air-stable lipid membranes have been applied in different systems such as hybrid bilayers [31], protein stabilized lipid bilayers [30], and polymerized membranes formed using synthetic diacetylene-containing phospholipids [32-34].

The advantages of this model are ease of preparation, stability, and patterning. In addition, numerous techniques are available for surface analysis such as atomic force microscopy, X-ray scattering, transmission electron microscopy, scanning electron microscopy, and Fourier transform infrared resonance [9]. However, the solid support affects the lipid bilayer and leads to

the loss of mobility and function for the incorporated membrane proteins. Moreover, membrane protein reconstitution is very challenging [4, 7, 9].

1.3.3. Nanodiscs

Nanodiscs are one of the newest class of model cell membrane and have shown to be an excellent tool for membrane protein studies. They are stable, self-assembled nano-structures of phospholipids encapsulated by an amphipathic protein defined and controllable size (Figure 1.3B) [35, 36]. The membrane scaffold protein (MSP) sequence can be tailored to create nanodiscs with different sizes (9.8 nm-17 nm) [37]. Nanodiscs are formed by addition of MSP to a detergent stabilized phospholipid and then using dialysis or adsorbtion to hydrophobic beads to remove the detergent [36-38]. Nanodiscs have several advantages including monodispersity, stability and consistency. They are also accessible from both sides of the membrane. However, the small size range of nanodisc that does not allow for the study of stoichiometric inclusion of multi-protein complexes.

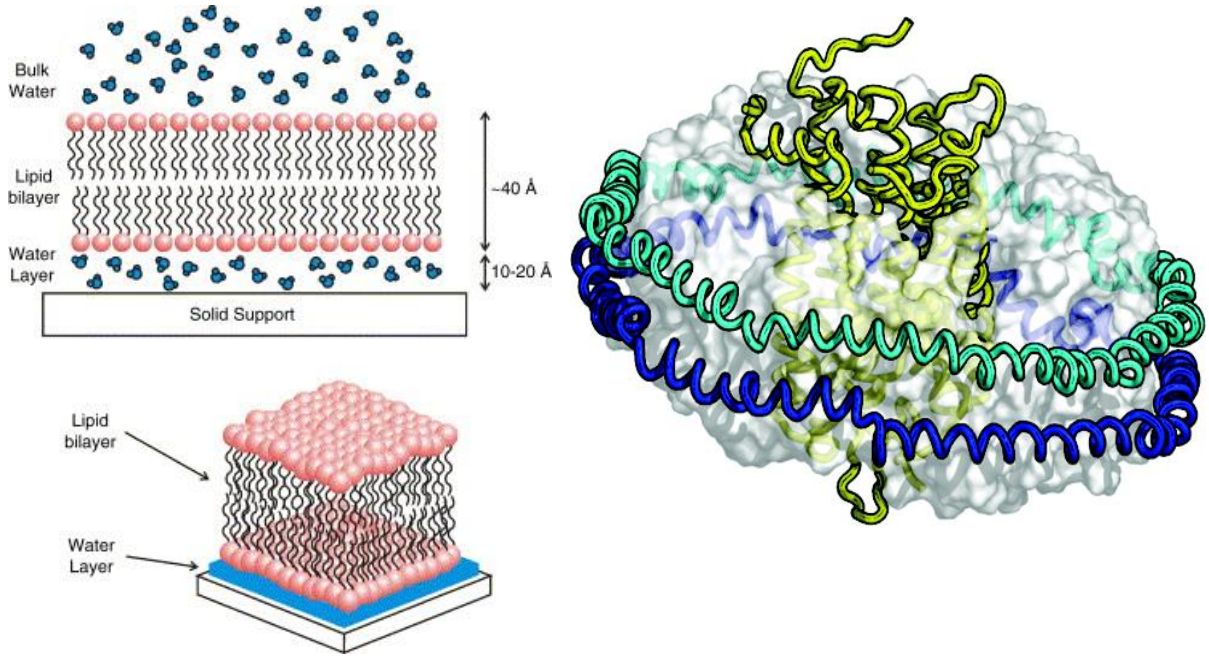

Figure 1.3. A schematic representation of (A) supported lipid bilayer [25] (B) Nanodisc [38]

1.3.4. Bicelles

Bicelles (or bilayered micelles) are generally formed by combination of long-chain phospholipids and short-chain phospholipids. These bilayered lipids were introduced in the 1990s and immediately became popular as a model membrane system due to their similarity with

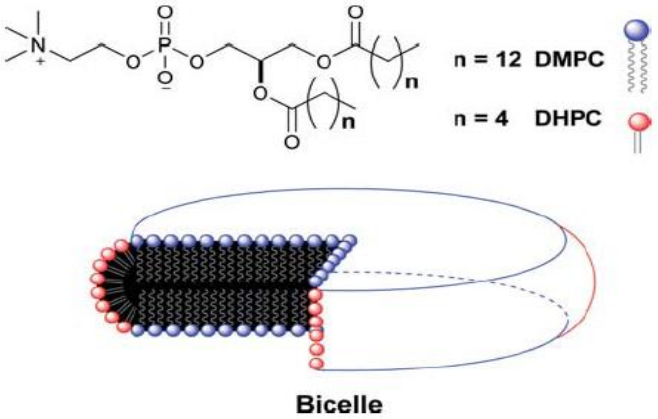

Figure 1.4. Schematic representation of the DMPC–DHPC bicelles [41]

biological membranes [39, 40]. Bicelles are disc-shaped structure morphology of long-chain and short-chain lipids which are concentrated at disc planar and rim, respectively (Figure 1.4) [41].

The combination of long-chain and short-chain phospholipids results in the formation of new structures with new morphology. The macroscopic structures of these morphologies have been thoroughly investigated resulting in establishing different phase diagrams. Small angle neutron scattering is used in order to draw a clear picture for all morphologies found in different research studies (Figure 1.5). The important factors in evaluating bicelle morphology are q, hydration level, temperature, and ionic strength.

When only long chain lipid is presented in the aqueous environment, multilamellar vesicles (MLV) are formed (Figure 5.1A). By adding detergent to solution, defects appear in the MLV structure due to low miscibility between lipid and detergent (Figure 5.1B).The vesicles start to collapse as the amount of detergent increases which result in formation of extended lamellae (Figure 5.1C) or chiral nematic ribbons (Figure 5.1D). Disc-shaped structures are formed when the content of detergent is higher (Figure 5.1E). The long-chain lipid forms a lipid bilayer in this morphology since it is still separated from the detergent. The detergent alone in the aqueous environment will form micelles (Figure 5.1F).

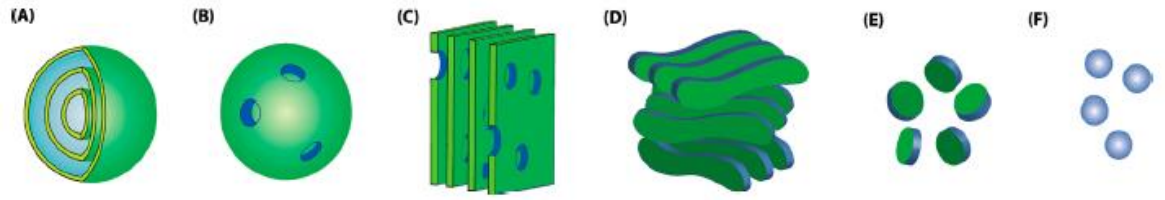

Figure 1.5. Schematic models for the morphology of bicellar phases with increasing detergent content: multilamellar vesicles (A), with toroidal pores lined up by detergents (B), extended lamellae showing magnetic-alignment (C), chiral nematic "worm-like" ribbons, also magnetically alignable (D), flat disk-like aggregates tumbling isotropically (E), and detergent micelles (F) [40]

The combination of dimyristoylphosphatidylcholine (DMPC), a long-chain, bilayer component, with dihexanoylphophatidylcholine (DHPC), a short-chain lipid, has been extensively recognized as the most popular option [41-44].

The significant factor in bicelle preparation is the ratio of long-chain to short-chain lipids, referred to as q (equation 1.1).

$$q = \frac{mole\ of\ long\ chain\ lipid}{mole\ of\ short\ chain\ lipid}$$ Equation 1.1

Bicelles have proved to be a more natural membrane environment in comparison with micelles. As their names suggest, bicelles have both features of bilayered vesicle and micelles. Their internal construction is composed of a bilayered lamellar structure, which is most important advantage of bicelles compared to micelles. Because of their improved characteristics, their use has been increased in recent studies [39, 42, 45, 46]. As it was mentioned before, the main disadvantage of vesicles as model membrane is lack of stability. Bicelles provide a stable environment for related studies. In addition, one of the challenging issues of SLB is the effect of

solid support on lipid properties such as mobility and function. In contrast, incorporation of protein in bicelles does not affect the characteristics of protein.

Different biophysical techniques such as nuclear magnetic resonance, X-ray crystallography, circular dichroism, and Fourier transform infrared spectroscopy are performed to study molecular interactions and structure of membrane peptides and proteins using the planar region of bicelles [22, 47-50]. Specifically, bicelles spontaneously orient in a magnetic field at high DMPC/DHPC molar (*q*) ratios (above 2.3) and within total lipid concentrations (3–60% w/v) and temperatures (30–50 °C) which is useful for solid-state NMR applications [48, 51-55].

Bicelles can be used in membrane protein studies in two ways using both isotropic and aligned bicelles. Membrane proteins are embedded in bicelles and solution-state or solid-state NMR spectroscopy are used for studies. In order to improve the result of NMR samples, different preparation protocols and all parameters need to be evaluated to find the optimum method and conditions. For instance, using the optimal q value in isotropically tumbling bicelles can result in distinguishing between mobile and structured residues in embedded proteins [56].

1.4.Poly-N-Substituted Glycines (Peptoids)

Peptoids, a type of peptidomimetics, are easy to synthesize, have low cost, diversity in side chain accessibility and resistance to proteolytic degradation. The backbone is similar to peptides with the side chains attached to the amide nitrogen rather than the α-carbon. Peptoids have two important characteristics that differentiate them from peptides: (1) lack of backbone chirality and (2) lack of backbone hydrogen bond donors (Figure 4A). These factors are the result of the modification to the backbone structure. Furthermore, appending the side chain to the amide

nitrogen results in a protease resistance backbone and a decreased immune response [57, 58]. The submonomer protocol for peptoid synthesis has advantages such as high coupling efficiencies and capability of adding a large diversity of side chain moieties due to the vast number of primary amines available [59].

The submonomer protocol has two stages: In the first stage, bromoacetic acid is utilized in order to acylate a secondary amine on the resin. In the second stage, a primary amine is added to the oligomer via an S_N2 reaction. These steps are repeated until the desired sequence is obtained (Figure 4B) [60]. After synthesise is complete, the peptoid is cleaved from the resin using trifluoroacetic acid.

Many studies have investigated the formation of peptoid secondary structure. Armand et al. used molecular modeling to predict that a stable helical structure can be formed by fully N-substituted glycines with aromatic and chiral side chain groups [61] which later was established via nuclear magnetic resonance [62]. Circular dichroism spectra of a peptoid with a polyproline type-I-like helix is similar to a peptide α-helix. The spectra has a maxima at 190 nm and two minima at 205 and 220 nm, respectively [63, 64]. In order to form robust helical structure, peptoid helices

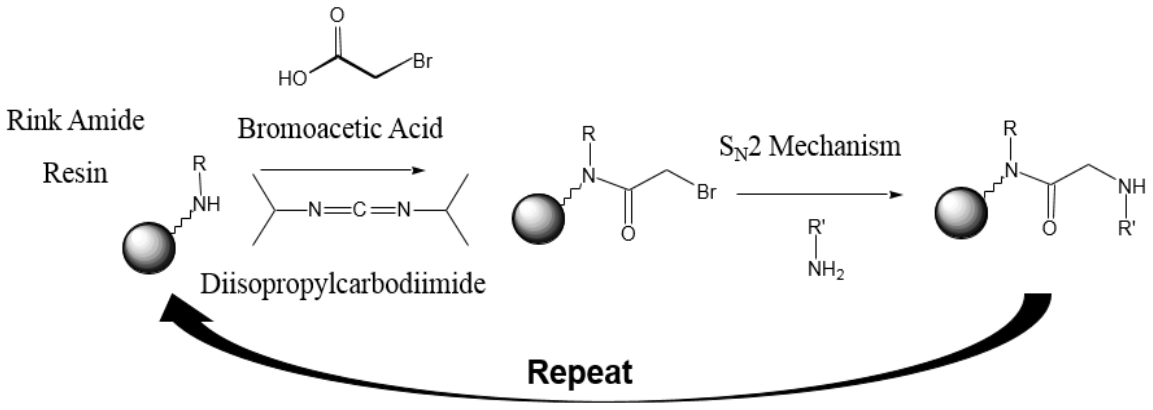

Figure 1.6. Peptoid submonomer synthesis protocol

should contain: (1) aromatic and chiral side chain (at least 50%), (2) C-terminus of the peptoid structure should be with a chiral, aromatic side chain, (3) one helical face should be composed of aromatic and chiral side chains [65, 66].

1.5.Interactions of Peptoids and Lipids

Peptoid/lipid interactions have previously been studied in the development of lung surfactant replacements. Peptide- and peptoid-based mimics of the lung surfactant proteins, SP-B and SP-C have been analyzed using the pulsating bubble surfactometer, Langmuir-Wilhelmy surface balance, and fluorescence microscopic film imaging [67-69]. However, the peptoid-based lung surfactant replacements were not able to mimic the surface activity of natural lung surfactant replacements. Another study has been shown that that lipid formulation composition is an important factor in the surface activity and structure of a specific SP mimic [70]. Therefore, in vitro function of two peptoid- and two peptide-based SP mimics in three different lipid formulations has been investigated in [71]. Moreover, the effects of side chain chemistry and length of the helical hydrophobic region in vitro testing of two classes of peptoid SP-C mimics have been evaluated [72]. Furthermore, a library of antimicrobial peptoids have been presented with different helical structures and biomimetic sequences [73].

1.6.Purpose and Significance of Research

Bicelles as a model cell membrane has been the focus of reserarchers since the 1990s and have a wide range of applications. Functionalizing bicelles with peptoids can provide applications in emerging areas such as drug delivery, biosensors, and bioseperations. Specifically, preferential edge modification of bicelle peptoids can be a promising alternative for peptdide modified

lipodisk as nanocarriers since use of PEG decreses the chance of getting approved by FDA. The product needs to be homogeneous to get approved by the FDA. However, the production process for PEG-protein conjugate are costly, difficult and inefficient [74-78]. Moreover, peptoid-funtionalilized bicelles can be anchored into gold nanoring arrays to develop biosensors. Peptoid-functionalized bicelles can also be applied in capillary electrophoresis as a media for membrane protein separation.

Chapter 2 Methods and Improvements

2.1. Synthesis of 2-tritysulfanyl-ethylamine

The protected thiol side chain, 2-tritysulfanyl-ethylamine, was prepared as previously described [79]. Briefly, triphenylmethanol was added to the solution of 2-aminoethanethiol hydrochloride in trifluoroacetic acid (TFA). Following incubation, the TFA was removed under reduced pressure using a rotating evaporator (Heidolph Laborota 4001, Elk Grove Village, IL). The solution was triturated with ethyl ether, the precipitant was partitioned with an aqueous solution of NaOH, and the product was extracted with ethyl acetate. The desired product was confirmed by ^{1}H NMR spectroscopy using a Bruker Avance 300 MHz spectrometer (Billerica, MA) equipped with a 5mm BBO probe and compared to previously published data (Figure 2.1) [80].

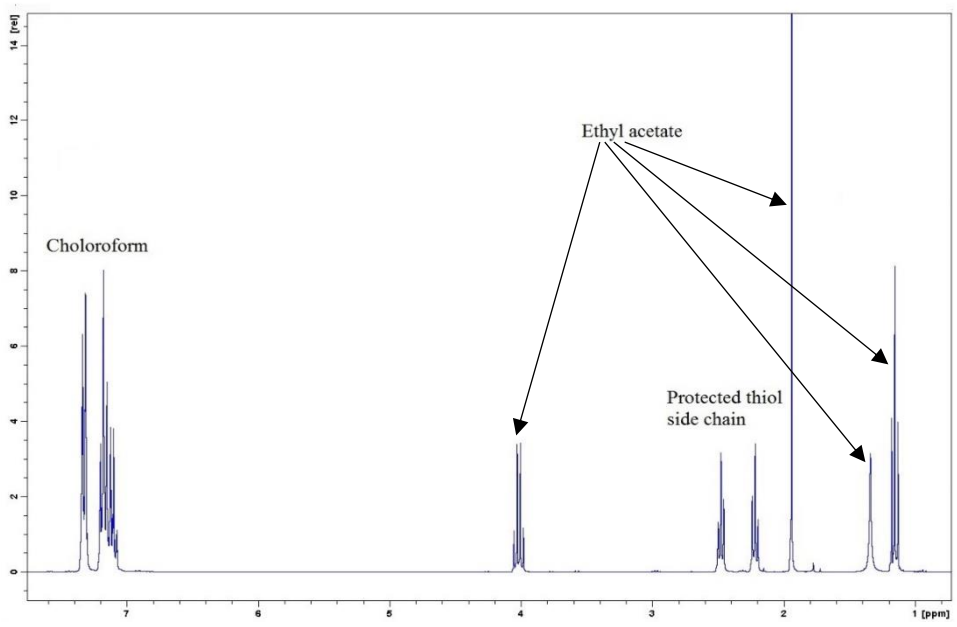

Figure 2.1. ^{1}H NMR spectra of the protected thiol side chain, 2-tritysulfanyl-ethylamine in deuterated dichloromethane. Chloroform and ethyl acetate spectra were the remaining from the synthesis process.

2.2. Peptoid Synthesis

Peptoids were synthesized *via* a submonomber solid-phase method using an Applied Biosystems 433A automated peptide synthesizer (Carlsband, CA) that was refurbished from a 431A synthesizer [59].Briefly, rink amide resin was swelled with dimethylformamide (DMF) and the Fmoc protecting group was removed using a 20% solution of piperidine in DMF. The two-step submonomer cycle starts with bromoacetylation by addition of 1.2 M bromoacetic acid in DMF and N, N'-diisopropylcarboniimide at a ratio of 4.3:1. In the next step, side chain were added to the resin *via* an SN2 reaction mechanism, which consists of incubation with 0.5-1 M amine in DMF for 90 min. The submonomer cycle was repeated until the desired sequence was achieved The peptoid was removed from the resin by bathing it in a solution of 95% trifluoroacetic acid (TFA), 2.5% triisoproylsilane, and 2.5% water for 10 min. The acid was removed using a Heidolph Laborota 4001 rotating evaporator (Elk Grove Village, IL) and the product was diluted to a concentration of ~3 mg/mL in a 50:50 solution of isopropanol-water.

2.3. Peptoid Purification

Peptoids were purified using preparative reversed-phase high pressure liquid chromatography (RP-HPLC; Waters Delta 600, Milford, MA) with a Duragel G C4 150 x 20 mm column (Peeke

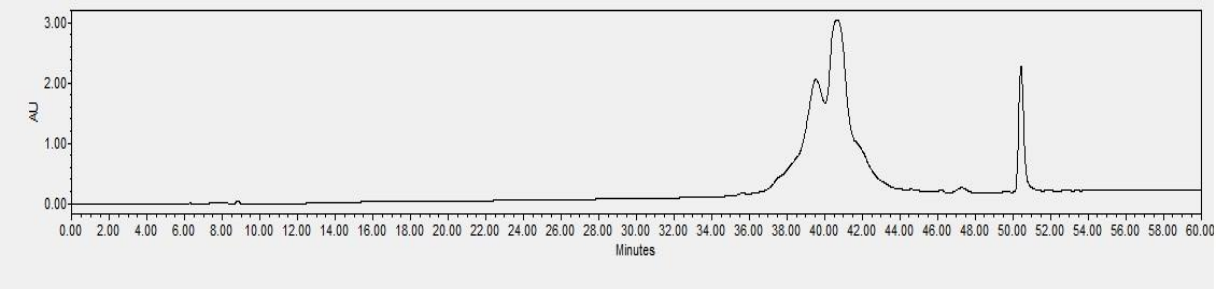

Figure 2.2. RP-HPLC chromatogram of Peptoid HN1

Scientific, Novato, CA). Gradients were run at ~1% per min with 30-70% solvent B in A (solvent A: water, 5% isopropanol, 0.1% TFA; solvent B: isopropanol, 5% water, 0.1% TFA) at room temperature.

2.4. Peptoid Characterization

Matrix-assisted laser desorption/ionization time of flight (MALDI-TOF) mass spectrometry (Bruker Daltonik GMBH, Bremen, Germany) was used to confirm that the purified peptoid molecular weight matched the theoretical mass calculated with ChemSketch (ACD/Labs, Toronto, ON). Peptoids were confirmed to be >98% pure via analytical HPLC (Waters 2695 Separations Module, Milford, MA) equipped with a Duragel G C4 150 x 2.1 mm column (Peeke Scientific, Novato, CA) using a linear gradient of 30 to 70% solvent D in C (solvent D: isopropanol, 0.1% TFA; solvent C: water, 0.1% TFA) over 30 min. Purified peptoid fractions were comibined and lyophilized using a Labconco lyophilizer (Kansas City, MO) and stored as a powder at -20 °C.

2.5. Circular Dichroism

Peptoid secondary structure was confirmed using CD spectrometry analysis to be a poly-proline type-I-like helix exhibits a maxima near 190 nm and two minima near 205 and 220 nm [65, 66, 81]. CD was performed using a Jasco J-1500 instrument (Easton, MD) at room temperature with a scanning speed of 50 nm/min and a path length of 0.2 mm. The peptoid was dissolved in pure methanol at a concentration of 430 μM and the CD spectra is the cumulative average of 10 scans.

2.6. Bicelle and Peptoid-functionalized Bicelles Preparation

Bicelles were prepared as previously described [82]. Briefly, chloroform was evaporated from the lipids using a gentle stream of nitrogen gas to form a lipid film, and the samples were placed under hard vacuum for 12 hr to ensure all solvent is removed. The long-chain lipid was incubated at room temperature for an additional 8 hr before hydration overnight with nanopure water to a final concentration of 0.38 mmole/mL. In order to form liposomes the hydrated long-chain lipid was incubated at 40 °C for 10 min, vortexed briefly, and placed in an 18 °C ice bath. This cycle was repeated ~3 times, until the solution was free-flowing when heated. The short-chain lipid was hydrated with nanopure water to a final concentration of 0.25 mmole/mL and vortexed at room temperature for 30 sec to form micelles. The desired molar ratio of long-chain (DMPC) to short-chain (DHPC) lipid, referred to as q [40], was combined. The lipid mixture (0.63 mmole/mL) was placed on ice for 5 min and vortexed for 1 min. The final step in bicelle formation consists of freezing using liquid nitrogen, and thawing in a 45 °C water bath. The freeze-thaw cycle was repeated ~10 times until the solution was transparent after being placed on ice for 5 min.

Peptoid-functionalized bicelles were prepared following two methods: (1) peptoid addition after bicelle formation and (2) peptoid addition before bicelle formation. Peptoid was dissolved in 50:50 solution of isopropanol and water. In order to prevent the formation of disulfide bonds, the reducing agent DTT was added to the peptoid solution at 1 mM prior to adding to the bicelle solution [83]. The preliminary results showed that Method 2 was successful in incorporating peptoid in the edge of bicelles. Therefore, Method 1 was chosen for the rest of the studies.

2.7. Transmission Electron Microscopy

Transmission electron microscopy (TEM) was used to visualize bicelles and peptoid-functionalized bicelles, as previously described [42, 45, 84, 85]. Briefly, TEM grids were prepared by dropping 5 μL of diluted bicelle solution onto a 300 square mesh formvar-carbon supported nickel (Method 1) or copper (Method 2) grid at room temperature. The grids were placed on filter paper to dry, stained with 2% uranyl acetate, and placed on filter paper to dry overnight. Images were obtained using a JEOL-1011 TEM (Tokyo, Japan) with an accelerating voltage of 110 kV. In order to obtain clear TEM images of the bicelles, samples were diluted with nanopure water [86]. Microsoft Visio was used to determine the diameter and thickness of the bicelles from the TEM images.

2.8. Gold Nanoparticle Studies

Gold nanoparticles (AuNP) were used to determine the location of peptoids within the bicelle structure. The AuNP size is 10±2 nm and the AuNP solution concentration is 40-50 μg/mL in water. First, 1.5 μL of non-functionalized and peptoid-functionalized bicelle solutions were combined with 1.0 mL of AuNP solution in 1.5 mL nanopure water [87] and then incubated for 1 hr on an orbital vortexer to allow for AuNP attachment to the thiols at the N-terminus of the peptoid [88-91]. AuNP-peptoid-functionalized bicelles were visualized by TEM without any further dilution, as described above.

2.9. Dynamic Light Scattering

The size of bicelles and peptoid-functionalized bicelles is an important parameter that needs to be measured. Dynamic light scattering (DLS) was performed, which uses the variation in

Brownian movement to measure the hydrodynamic diameter of particles in solution assuming a spherical shape [92]. The hydrodynamic radius was translated to the radius of a disc for the bicelles using Equation (2.1) [93],

$$Rh = \frac{3}{2} r \left(\left[1 + \left(\frac{t}{2r} \right)^2 \right]^{1/2} + \frac{2r}{t} Ln \left[\frac{t}{2r} + \left[1 + \left(\frac{t}{2r} \right)^2 \right]^{1/2} \right] - \frac{t}{2r} \right)^{-1} \quad \text{Equation 2.1}$$

where Rh is hydrodynamic radius, r is disc radius, and t is disc thickness determined by TEM. The experiments were carried out at 25 °C using a Delsa™Nano C (Beckman Coulter, Brea, CA). The bicelle solutions were diluted with nanopure water.

Chapter 3 Altering the Edge Chemistry of Bicelles with Peptoids

3.1. Introduction

Biological membranes draw a boundary between or within cells and organelles, enabling the isolation of different cellular processes during tightly regulated transportation of materials into and across membranes [1]. They also serve as a home for biochemical processes since many physiological events, such as signaling, fusion, and fission, occur in the membrane. Membranes have a complex composition, including both lipid and protein, and are dynamic in nature. The main class of membrane lipids is phospholipids, which consist of two hydrophobic fatty acid chains linked to a phosphate-containing hydrophilic head group. Due to their amphipathic character, phospholipids form bilayers in aqueous solutions [94]. Investigating the nature of cell membranes and their reciprocal relationships is very challenging, specifically when trying to establish membrane biology in non-natural systems. Due to the complexity of biological membranes, a vast number of modified, but similar, model systems with precise size, geometry, and composition have been developed to investigate membrane characteristics, lipid-lipid interactions, and drug discovery and delivery [4, 7-9]. Many model membrane systems preserve the structure and function of the lipid bilayer, while simplifying the system to evaluate the role of each component and visualize the organization and function of the system. Commonly used model membrane systems include: vesicles [3, 9, 95, 96], supported lipid bilayers [97-99], nanodiscs [37, 38, 100, 101], and bicelles [40, 42, 43, 45, 102, 103].

Vesicles are lipid bilayers of phospholipids [104], and are typically formed by slow evaporation from volatile organic solvents and resuspension in an aqueous solution [20]. While vesicles have fundamental similarity to the biological cell membrane and are easy to prepare, they are limited

by low stability and the ability of incorporated proteins to interact with each other [7, 20, 21]. Supported lipid bilayers are flat membranes that are created on a hydrophilic support such as mica, glass, or silica by lipid vesicle fusion or using the Langmuir-Blodgett technique, and often have a very thin (~5 Å) aqueous layer between the solid support and the lipid membrane [4, 9]. The advantages of supported lipid layers are their ease of preparation, stability, and their ability to incorporate patterning. However, surface effects impair protein stability and decrease lipid mobility [7, 105].

Bicelles and nanodiscs are disc-shaped lipid bilayers that are accessible from both sides, unlike the previously discussed lipid structures. Nanodiscs contain phospholipids in the planar, bilayer surface and an engineered, amphipathic, helical membrane scaffold protein at the edge [36, 37, 101]. These self-assembled structures provide high stability, access to both sides of the membrane, and monodispersity [36]. However, nanodiscs have a small, uniform size range (8 to 13 nm) that does not permit the study of stoichiometric inclusion of multi-protein complexes [106].

Bicelles are formed by combining long-chain and short-chain lipids, where the long-chain lipids form the planar surface of the disc and the short-chain lipids form the edge [40]. These bilayered lipid discs have been investigated as a model membrane system due to their similarity to biological membranes in lipid composition and their planar surface [39, 46]. Bicelles overcome the issues of stability and mobility that impair vesicles and supported lipid bilayers, while maintaining the structure and function of incorporated proteins [16, 18, 20, 21]. The size of bicelles can be custom-tailored, resulting in a wide range of sizes (10-100 nm), thereby overcoming the concerns of nanodiscs [40, 102, 107]. The main shortcoming of bicelles is their

limited temperature and hydration levels in the bicellular phase diagram. Efforts that have been made to extend the bicellar region include the use of designed lipids with biphenyl-containing acyl chains and stabilizing the bicelles by the addition of sialylated lipids [40].

Bicelles have been previously modified with poly(ethylene glycol) (PEG), which created a new class of model cell membrane called lipodisks [108-110]. In lipodisks, the PEGylated lipids are mostly at the edges of the bicelle improving stability for the investigation of drug-membrane interactions and drug partition studies [74, 111]. In recent studies, lipodisks have shown promise as nanocarriers. The rim of lipodisks has high affinity to amphiphilic peptides with antimicrobial and anticancer activity and can be easily modified with peptides [74, 112]. Peptide-modified lipodisks have been developed as a tumor-targeted drug delivery system for potential anticancer candidate, such as melittin [75, 76]. However, PEGylated protein drugs have to meet several criteria in order to get FDA approval [77].

The focus of this study is to modify the edge chemistry of bicelles through incorporation of peptoids, peptide-like molecules that have their side chain attached to the backbone amide rather than the alpha-carbon [58]. Functionalizing bicelles with peptoids leads to applications in biosensors, bioseperations, and drug delivery. Peptoid-functionalized bicelles can be customized to bind to gold nanoring arrays for use in biosensors. Peptoid-functionalized bicelles can also be used as a media for membrane protein separation in capillary electrophoresis to increase yield. Moreover, peptoid-functionalized bicelles are an interesting alternative for peptide-modified lipodisks with eliminating the need for PEG with the better chance of getting approved by the FDA. Peptoids are useful in this application because a large diversity of side chains are available, and they are sequence-specific, easy to synthesize and, resistant to proteolytic degradation, and

elicit a low immune response [59]. Peptoids are synthesized via a submonomer protocol that yields high coupling efficiencies compared to peptides [60] and a large diversity of side chain moieties are available as primary amines [58].While peptoids lack backbone chirality and hydrogen bond donors, a secondary structure can be introduced through side chain chemistry [61, 113]. For example, peptoids with chiral, aromatic side chains form robust polyproline type-I-like helices with ~6 A° pitch and 3 monomers per turn [62]. These helices are stabilized by steric interactions, rather than hydrogen bonds, leading to stable secondary structure even with increasing temperature and inclusion of denaturants such as urea [66].

The interaction of peptoids and lipids has been studied for biomedical applications including lung surfactant mimics, antimicrobials, and cellular uptake and delivery [65-69, 72, 73, 114-121]. Barron and co-workers designed and characterized amphipathic peptoids as mimics of lung surfactant proteins and showed that the facially and longitudinally amphipathic helices insert into the lipid layer [65-69, 72, 114-116]. Further studies showed that the inclusion of alkyl side chains improves insertion of the peptoids into the lipid layer [114, 115]. Peptoid-based mimics of antimicrobial peptides have been shown to decrease bacterial cell growth [119], and molecular studies confirm that the peptoid helices interact with lipids in a similar manner as antimicrobial peptides [73]. Zuckerman et al. first used cationic peptoids conjugated to phospholipid headgroups (lipitoids) as cellular uptake agents [120]. The protease-resistance feature of peptoids makes the lipitoids a group of synthetic polymers that has shown promising results in *in vitro* cellular delivery of plasmid DNA [121].

Here we report, for the first time, the functionalization of bicelle edges with peptoid HN1. These studies show that peptoid functionalization does not significantly alter bicelle morphology or

size, and that the amphipathic peptoid preferentially incorporates into the edge of the bicelles. These findings indicate that peptoids can be used to modify the edge chemistry of bicelles with

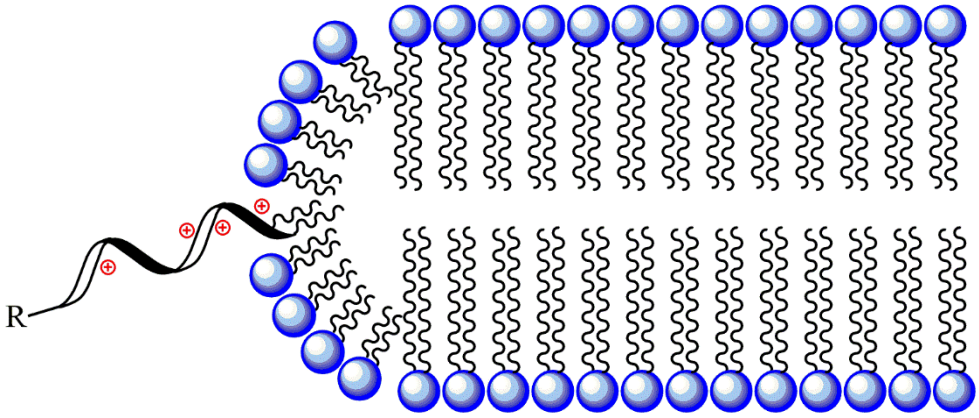

Figure 3.1. Schematic representation of peptoid-functionalized bicelles

potential applications in biosensors and bioseparations.

3.2. Materials and Methods

3.2.1. Materials

1,2-dimyristoyl-sn-glycero-3-phosphocholine (DMPC; 14:0 PC) and 1,2-dihexanoyl-sn-glycero-3-phosphocholine (DHPC; 6:0 PC) dissolved in chloroform were purchased from Avanti Polar Lipids (Alabaster, AL). MBHA rink amide resin was purchased from NovaBiochem (Gibbstown, NJ), piperidine was purchased from Sigma-Aldrich (St. Louis, MO), hexylamine and S-methylbenzylamine were purchased from Acros Organics (Pittsburgh, PA) and tert-butyl N-(4-aminobutyl)carbamate was purchased from CNH Technologies Inc. (Woburn, MA). Gold nanoparticles (AuNP) in aqueous solution were purchased from NNCrystal (Fayetteville, AR), and carbon-coated copper grids 300 mesh TYPE A and carbon-coated nickel grids 300 mesh were purchased from Ted Pella. Inc. (Redding, CA). All other reagents and materials were

purchased from VWR. All chemicals were used without further modification, unless otherwise noted.

3.2.2. Synthesis of 2-tritysulfanyl-ethylamine

The protected thiol side chain, 2-tritysulfanyl-ethylamine, was prepared as previously described [79]. Briefly, triphenylmethanol was added to the solution of 2-aminoethanethiol hydrochloride in trifluoroacetic acid (TFA). Following incubation, the TFA was removed under reduced pressure using a rotating evaporator (Heidolph Laborota 4001, Elk Grove Village, IL). The solution was triturated with ethyl ether, the precipitant was partitioned with an aqueous solution of NaOH, and the product was extracted with ethyl acetate. The desired product was confirmed by ^{1}H NMR spectroscopy using a Bruker Avance 300 MHz spectrometer (Billerica, MA) equipped with a 5mm BBO probe and compared to previously published data [80].

3.2.3. Peptoid Synthesis and Purification

Peptoid HN1 was synthesized following a submonomer method [59] using an ABI 433A automated peptide synthesizer that was refurbished from a 431A synthesizer (Carlsband, CA), as previously described [122]. Briefly, rink amide resin was swelled by bathing it in dimethylformamide (DMF) and the Fmoc protecting group was removed using 20% piperidine in DMF. The submonomer cycle consists of (1) the addition of 1.2 M bromoacetic acid in DMF and N, N'-diisopropylcarboniimide at a ratio of 4.3:1 and (2) incubation with 0.5-1 M amine in DMF for 90 min. The submonomer cycle was repeated until the desired sequence was obtained. Peptoid HN1 was cleaved from the resin by incubation in a mixture of 95% TFA, 2.5% water, and 2.5% triisopropylsilane for 10 min. The resin was filtered from the peptoid solution, the TFA

was removed using a rotating evaporator, and the product was dissolved in 50:50 isopropanol:water to a final concentration of ~3 mg/mL.

Peptoid HN1 was purified by preparative reversed-phase high pressure liquid chromatography (RP-HPLC; Waters Delta 600, Milford, MA) with a Duragel G C4 150 x 20 mm column (Peeke Scientific, Novato, CA). Gradients were run at ~1% per min with 30-70% solvent B in A (solvent A: water, 5% isopropanol, 0.1% TFA; solvent B: isopropanol, 5% water, 0.1% TFA) at room temperature. Peptoid purity of >97% was confirmed using a Waters 2695 separations module analytical RP-HPLC with a Duragel G C4 150 x 2.1 mm column (Peeke Scientific) and a linear gradient of 30 to 70% solvent D in C over 60 min (solvent C: water, 0.1% TFA; solvent D: isopropanol, 0.1% TFA). The molecular weight of the peptoid was determined using matrix-assisted laser desorption/ionization (MALDI) mass spectrometry (Bruker Daltonik GMBH, Bremen, Germany) and compared to the molecular weight calculated with ChemSketch (ACD/Labs, Toronto, ON) (Supporting information, Figure S3.1). The formation of peptoid dimer was confirmed by MALDI and analytical RP-HPLC which showed that a reducing agent was required [83]. Purified peptoid solutions were dried to powder using a Labconco lyophilizer (Kansas City, MO) and stored at −20 °C until use.

3.2.4. Circular Dichroism

The secondary structure of peptoid HN1 was confirmed to be a poly-proline type-I-like helix by circular dichroism (CD; Supporting information, Figure S3.2). CD spectroscopy analysis was performed using a Jasco J-1500 instrument (Easton, MD) with a scanning speed of 50 nm/min and a path length of 0.2 mm at room temperature. The peptoid was dissolved in pure methanol at

a concentration of 430 μM and the CD spectra is the cumulative average of 10 scans. Data are presented as per residue molar ellipticity.

3.2.5. Bicelle and Peptoid-Functionalized Bicelle Preparation

Bicelles were prepared as previously described [82]. Briefly, chloroform was evaporated from the lipids using a gentle stream of nitrogen gas to form a lipid film, and the samples were then placed under hard vacuum for 12 hr to remove all solvent. The long-chain lipid was incubated at room temperature for an additional 8 hr before hydration overnight with nanopure water to a final concentration of 0.38 mmole/mL. In order to form liposomes, the hydrated long-chain lipid was incubated at 40 °C for 10 min, vortexed briefly, and placed in an 18 °C ice bath. This cycle was repeated ~3 times, until the solution was free-flowing when heated. The short-chain lipid was hydrated with nanopure water to a final concentration of 0.25 mmole/mL and vortexed at room temperature for 30 sec to form micelles. A 1.5:1 molar ratio of long-chain (DMPC) to short-chain (DHPC) lipid, referred to as q [40], was used for these studies. The lipid mixture (0.63 mmole/mL) was placed on ice for 5 min, vortexed for 1 min, frozen using liquid nitrogen, and thawed in a 45 °C water bath. The freeze-thaw cycle was repeated ~10 times until the solution was transparent after being placed on ice for 5 min.

Peptoid-functionalized bicelles were prepared following two methods: (1) peptoid addition after bicelle formation and (2) peptoid addition before bicelle formation. Peptoid was added at 0.25 or 20 mole% of the short-chain lipid (DHPC). In order to prevent the formation of disulfide bonds, the reducing agent DTT was added to the peptoid solution at 1 mM prior to adding to the bicelle solution [83]. Peptoid-functionalized bicelles prepared in the absence of DTT formed aggregates due to disulfide bonds, as observed by TEM and DLS (Supporting information, Figure S3.3).

3.2.6. Transmission Electron Microscopy

Bicelles and peptoid-functionalized bicelles were visualized by TEM, as previously described [42, 45, 84, 85]. TEM grids were prepared at room temperature by dropping 5 μL of diluted bicelle solution onto a carbon-coated copper (for Method 1) or carbon-coated nickel (for Method 2) grid. The grids were placed on filter paper to dry, stained with 2% uranyl acetate, and placed on filter paper to dry overnight. Images were obtained using a JEOL-1011 TEM (Tokyo, Japan) with an accelerating voltage of 110 kV. Microsoft Visio was used to determine the diameter and thickness of the bicelles from the TEM images.

In order to obtain clear TEM images of the bicelles, samples were diluted with nanopure water to final lipid concentrations of 6.36, 3.18, 0.318, and 0.159 mM for bicelles and 0.183, 0.091, 0.009, and 0.005 mM for peptoid-functionalized bicelles [86]. It was determined that samples with a final lipid concentrations of 0.159 mM non-functionalized bicelles and 0.005 mM peptoid-functionalized bicelles resulted in the best images (Supporting information, Figure S3.4).

3.2.7. Dynamic Light Scattering (DLS)

DLS was used to determine the size distribution of bicelles and peptoid-functionalized bicelles in solution. DLS uses the variation in Brownian movement to measure the hydrodynamic diameter of particles in solution, assuming a spherical shape [92]. The hydrodynamic radius was translated to the radius of a disc for the bicelles using Equation (3.1) [93],

$$Rh = \frac{3}{2} r \left(\left[1 + \left(\frac{t}{2r} \right)^2 \right]^{1/2} + \frac{2r}{t} Ln \left[\frac{t}{2r} + \left[1 + \left(\frac{t}{2r} \right)^2 \right]^{1/2} \right] - \frac{t}{2r} \right)^{-1} \quad \text{Equation 3.1}$$

where Rh is hydrodynamic radius, r is disc radius, and t is disc thickness determined by TEM. The experiments were carried out at 25 °C using a Delsa™Nano C (Beckman Coulter, Brea, CA). The bicelle solutions were diluted with nanopure water.

3.2.8. Determination of Peptoid Position

The location of peptoid HN1 within the bicelles was determined by incubation with AuNP. The AuNP size is 10±2 nm and the AuNP solution concentration is 40-50 µg/mL. 1.5 µL of non-functionalized and peptoid-functionalized bicelle solutions were combined with 1.0 mL of AuNP solution in 1.5 mL nanopure water [87] and incubated for 1 hr on an orbital vortexer to allow for AuNP attachment to the thiols at the N-terminus of peptoid HN1 [88-91]. AuNP-peptoid-functionalized bicelles were visualized by TEM without any further dilution, as described above.

3.3. Results and Discussion

3.3.1. Peptoid HN1 Sequence and Rationale

The ability to selectively alter the surface chemistry of bicelles will lead to improved function as model cell membranes in applications such as biosensors and electrophoretic separations. Previous studies showed that peptoids can be designed to interact with lipids [67, 72, 115] and, in some cases insert into lipid structures [68, 69] and anchor into the lipid membrane [114].

Peptoid HN1 sequence reported here is based on work in the Barron lab that showed that alkylation of a cationic, facially amphipathic peptoid led to improved insertion into lipid films [114]. Specifically, peptoid HN1 reported here has three functional regions (Figure 1): (1) insertion sequence, (2) facially amphipathic helix (charged anchor), and (3) functional groups. The insertion region includes two alkyl chains that match the length of the DHPC tail groups that make up the bicelle edge (6 carbons) and two hydrophobic, chiral aromatic groups. This region of the peptoid inserts into the hydrophobic lipid tail region and serves as an anchor into the bicelle edge. The facially amphipathic helix contains chiral aromatic groups to induce helical

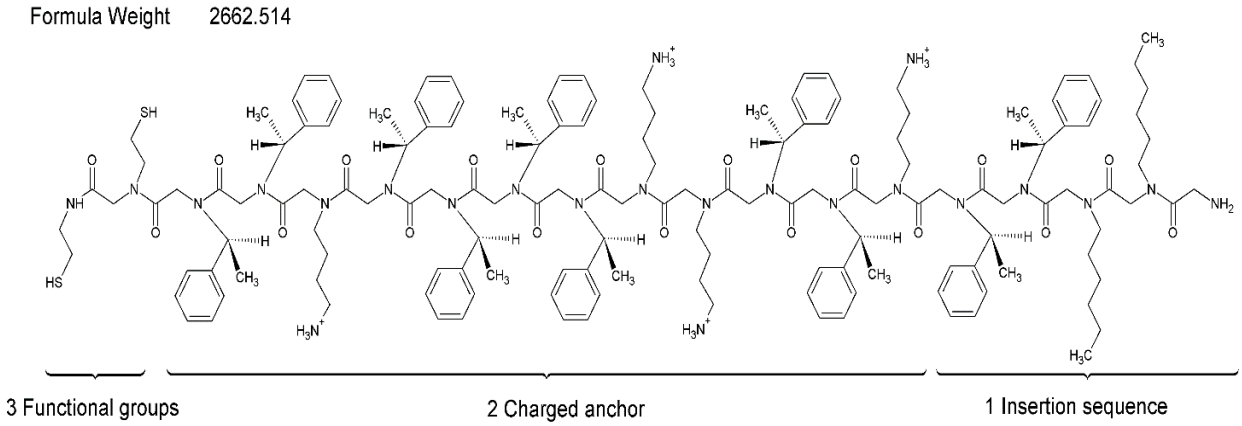

Figure 3.2. Peptoid HN1 structure and molecular weight. There are 3 active regions on the peptoid: (1) insertion sequence, (2) charged anchor, and (3) functional groups.

secondary structure with three residues per turn [62]. One side of the helix is hydrophobic to interact with the lipid tails, and the other side contains positive charges to interact with the lipid head groups. The functional group selected for this study was thiol to allow for AuNP attachment to determine peptoid location within the bicelle.

3.3.2. Effect of Peptoid on Bicelles

Bicelles were composed of DMPC and DHPC (C14 and C6, respectively) with 0, 0.25, or 20 mole% peptoid HN1, relative to DHPC. Peptoid-functionalized bicelles were prepared by adding

peptoid HN1, either after bicelle formation (Method 1) or before bicelle formation (Method 2). Bicelle morphology and size were determined by TEM imaging for non-functionalized and peptoid functionalized bicelles. In the absence of peptoid HN1, bicelles in both face-on and edge-on projections were observed by TEM imaging (Figure 2A) with an average diameter of 36.5±13.0 nm, in accordance with previously published data for DMPC:DHPC bicelles [41, 123-125].Bicelles prepared with 0.25 mole% peptoid HN1 by Method 1 had similar morphology to non-functionalized bicelles, with an average diameter of 48.4±12.0 nm (Figure 2B). Bicelles prepared with 20 mole% peptoid HN1 by Method 1 formed aggregates that required further dilution of the bicelle solution to obtain clear images. At the higher peptoid HN1 concentration, a layer of bicelles was observed with peptoid HN1 aggregates on top (Figure 2C). The average diameter for the peptoid-functionalized bicelles and small peptoid HN1 aggregates was 28.1±5.3 nm. Peptoid-functionalized bicelles prepared by Method 2 had morphology similar to non-functionalized bicelles for both the 0.25 and 20 mole% peptoid HN1concentrations (Figures 2E and 2F). The average diameter of the bicelles was 47.8±14.4 nm for 0.25 mole% peptoid HN1

and 48.6±11.2 nm for 20 mole% peptoid HN1. Bicelle size in nanopure water solution was determined by DLS for non-functionalized and peptoid-functionalized bicelles. The measured hydrodynamic radius of the particles was transformed to the disc radius using Equation 1 using a bicelle thickness of 5.4 nm as determined by TEM, which is in agreement with previously published data [45, 103]. DLS results show that in the absence of peptoid HN1, the bicelles had a diameter of 31.8±20.5 nm in solution, in agreement with previous studies [45, 126].

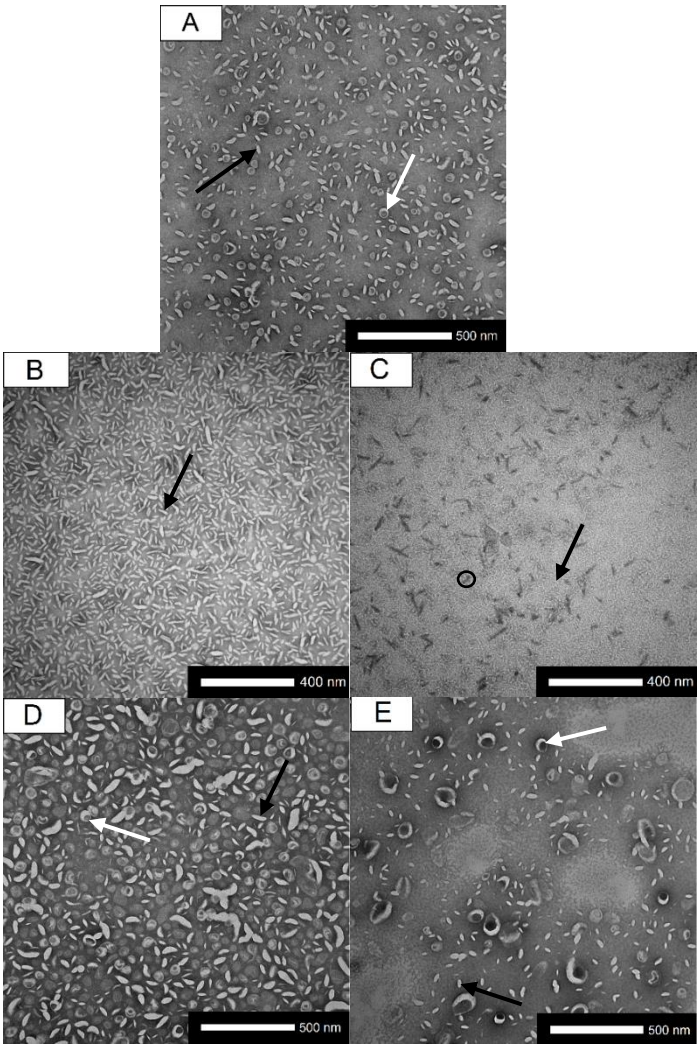

Figure 3.3. TEM images of non-functionalized (A) and peptoid-functionalized bicelles prepared by Method 1 (B and C) or Method 2 (D and E) with peptoid-DHPC = 0.25 mole% (B and D) or 20 mole% (C and E) and q=1.5. Face-on bicelles are indicated by white arrows, edge-on bicelles are indicated by black arrows, and peptoid HN1 aggregates are indicated by black circles. Scale bar represents 500 nm (A, D, E) or 400 nm (B, C).

For peptoid-functionalized bicelles prepared by Method 1 with 0.25 mole% peptoid HN1, the average diameter was 45.5±15.1 nm (Figure 3A). When the peptoid HN1 concentration was increased to 20 mole%, two peaks appeared on the size distribution curve: (1) a peak for peptoid-functionalized bicelles and small peptoid HN1 aggregates with an average diameter of 26.41±16.40 nm and (2) a peak for larger peptoid HN1 aggregates with an average diameter of 76.35±30.84 nm. DLS results for the peptoid-functionalized bicelles prepared using Method 2 showed no aggregates (Figure 3B) and had an average diameter of 47.8±14.4 nm for 0.25 mole% peptoid HN1 and 48.6±11.2 nm for 20 mole% peptoid HN1.

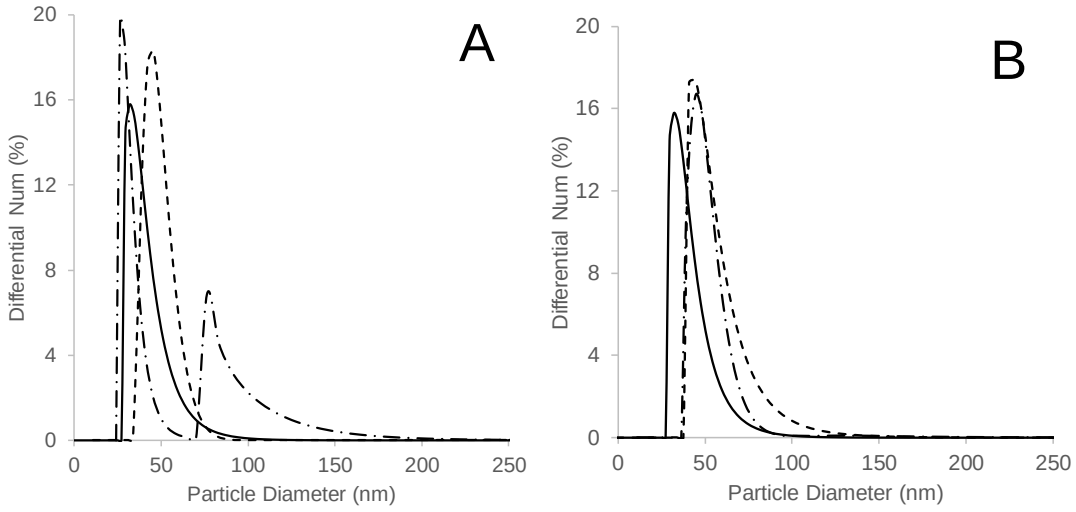

Figure 3.4. DLS size distribution curves for non-functionalized (solid) and peptoid-functionalized bicelles with 0.25 mole% (dash) or 20 mole% (dash-dot-dash) prepared by Method 1 (A) and Method 2 (B) with q = 1.5. The hydrodynamic radius was transformed to the disc radius using equation 1.

3.3.3. Placement of peptoid within bicelles

The position of the peptoid within the bicelle was determined by incubation with AuNP, which interacted with the thiol groups at the N-terminus of peptoid HN1, followed by visualization with TEM. Incubation of AuNP with non-functionalized bicelles confirmed that the AuNPs did not interact with bicelles without peptoid (Supporting information, Figure S3.5). Additionally, AuNPs had limited interaction with peptoid-functionalized bicelles containing 0.25 mole% peptoid (Supporting information, Figure S3.5). All further studies to determine peptoid position in the bicelle were completed with 20 mole% peptoid HN1.

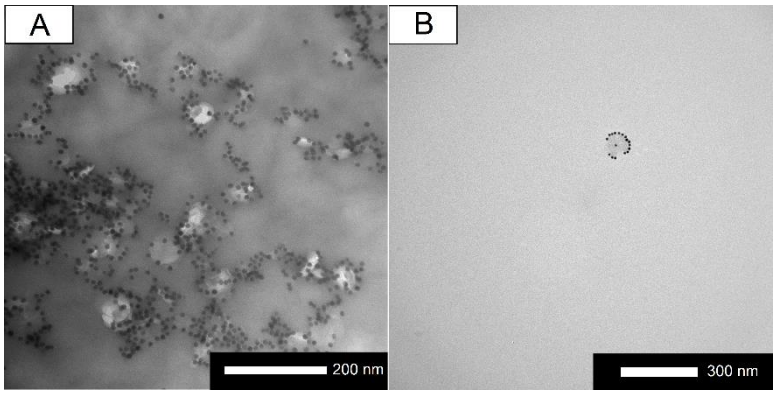

Figure 3.5. TEM images of AuNP modified peptoid-functionalized bicelles with peptoid-DHPC = 20 mole% and q=1.5 prepared by Method 1 (A) or Method 2 (B)

TEM images of AuNP-peptoid-functionalized bicelles prepared by Method 1 showed that the peptoid was incorporated in both the bicelle face and edge with little preference (Figure 4A). Quantitative analysis of the TEM images revealed that 54% of the peptoid was incorporated into the edge of the bicelle. AuNP incubation with peptoid-functionalized bicelles prepared by Method 2 showed preferential incorporation of peptoid into the bicelle edges (Figure 4B). TEM image analysis showed 82% peptoid incorporation into the bicelle edge, as opposed to the face. The incorporation of some peptoid into the face is not surprising considering that previous

studies showed that the non-idealized molecular structure of bicelles leads to the presence of some DHPC molecules in the face of the bicelle [102, 127].

3.4.Discussion

Here we report the successful formation of bicelles functionalized with peptoid preferentially at the edges. TEM results show that discoidal peptoid-functionalized bicelles were formed by Method 2 with both 0.25 and 20 mole % peptoid, at 0.25 mole % peptoid for Method 1. The main difference between two methods is the peptoid addition step. In Method 2, peptoid incorporate into the bicelle structure along with the lipids since peptoid was added during the bicelle formation. In fact, peptoid is a part of self-assembly process of bicelle formation. The insertion region of peptoid which contains alkyl chain matching the length of the DHPC tail groups, preferentially assembled with the DHPC at the edges of bicelle. The results for 5% and 20% mole peptoid show that disc-shaped structure of bicelle was the only observed morphology and the addition of peptoid does not alter the discoidal bicelle shape. Preferential incorporation of the peptoid into the bicelle edge was confirmed by attachment of AuNPs to the thiol groups on the N-terminus of the peptoid. Peptoid-functionalized bicelles prepared by Method 2 showed preferential placement in the bicelle edge (~80%). In Method 2, addition of peptoid before bicelle formation allows the insertion region of peptoid incorporates preferentially into the edges of the bicelle. The insertion of peptoid in the planar region of bicelle is minor, but predictable, since the alkyl chain length of peptoid is shorter than the length of the DMPC tail groups.

In Method 1, peptoid was added after bicelles were already formed. The peptoid is not a part of self-assembly process of bicelle formation. At 5% mole peptoid for Method 1, only disc-shaped structure of peptoid-functionalized bicelles was observed. However, as the peptoid concentration

was increased to 20 mole %, three morphologies were observed including peptoid-functionalized bicelles, small peptoid aggregates, and larger peptoid aggregates. These results show at 20 mole% peptoid, the amount of peptoid is high and since the peptoid addition is not a part of self-assembly process, peptoid molecules started to interact with each other and formed aggregates. Therefore, peptoid-functionalized bicelles were formed but also peptoid aggregation occurred. AuNPs studies show bicelles formed by Method 1 showed no preference for the edge versus the face (~50%)

Preferential incorporation of the peptoid into the bicelle edge was confirmed by attachment of AuNPs to the thiol groups on the N-terminus of the peptoid. Peptoid-functionalized bicelles prepared by Method 2 showed preferential placement in the bicelle edge (~80%), whereas the bicelles formed by Method 1 showed no preference for the edge versus the face (~50%). In Method 2, addition of peptoid before bicelle formation allows the insertion region of peptoid incorporates preferentially into the edges of the bicelle. While forming peptoid-functionalized bicelles by method 1, bicelles are already formed and when peptoids are added, they incorporated into any available space, so there is no preference.

Size analysis performed using DLS and TEM images not only show agreement between the two methods, but also show no statistical difference in bicelle diameter with the addition of peptoid, based on ANOVA analysis (Table 1). The average particle diameter for peptoid-functionalized bicelles was larger than the diameters of bicelles alone, likely due to peptoid incorporation in the edges of the bicelles.

Table 3.1. Comparison between particle diameter based on TEM images analysis and DLS

mole% peptoid in DHPC		**Peptoid-functionalized bicelles diameter (nm)**	
		TEM images analysis	**DLS**
0		36.55±13.00	31.82±20.48
Method 1	0.25	48.35±11.95	45.53±15.14
	20	-	-
Method 2	0.25	47.84±14.36	44.15±27.79
	20	48.61±11.16	44.69±14.64

3.5.Conclusions

To our knowledge, this is the first time bicelles have been functionalized with peptoids to modify the edge chemistry. Peptoids are promising candidates for bicelle functionalization since they are easily synthesized, sequence-specific, resistant to proteolytic degradation, and have a vast number of side chains available for synthesis. The insertion of peptoids into the edges of bicelles alters the surface chemistry and creates interaction regions for membrane protein studies with potential applications in biomarker detection and drug discovery. Peptoid-functionalized bicelles can also be used as a media for capillary electrophoresis, which may increase the yield in membrane proteins separation processes [128, 129], and can help to improve the selectivity for drug screening processes. Further studies may focus on using different q values, peptoid sequences, and other lipid combinations to investigate these effects on bicelle size and stability.

3.6.Supporting Information

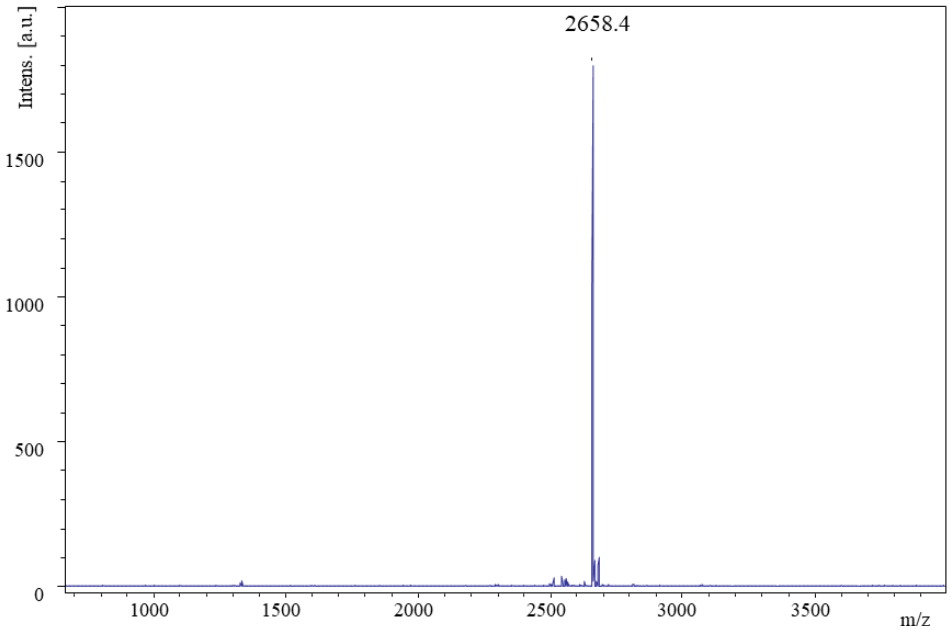

Figure S3.1. MALDI-TOF mass spectrometry was used to confirm that the purified peptoid mass matched the theoretical mass.

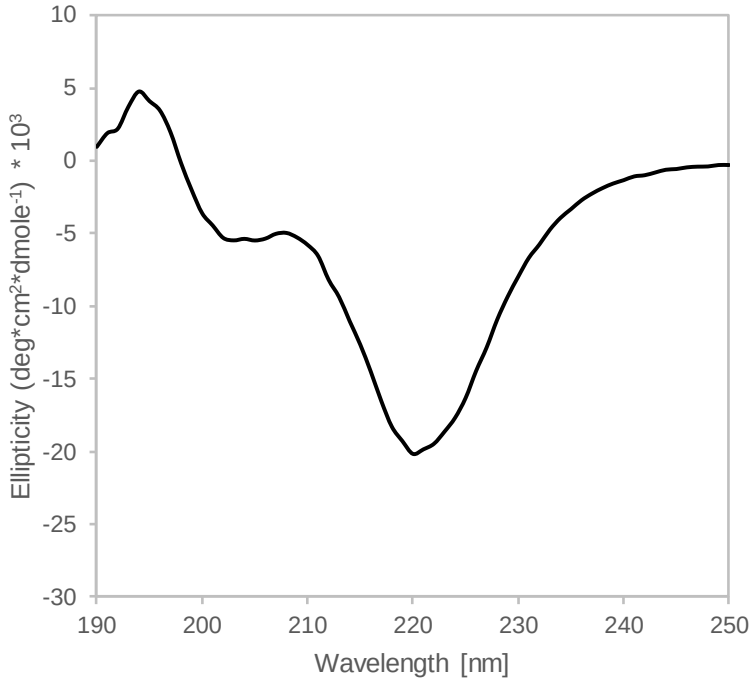

Figure S3.2. Circular dichroism spectra for the peptoid. The spectra depict a polyproline type I-like helical secondary structure. The CD spectra exhibits a characteristic maximum near 193 nm and two minima near 205 and 220 nm [24, 47-49].The increased intensity of the 220 nm peak as compared to the 205 nm peak is indicative of a stable helical secondary structure.

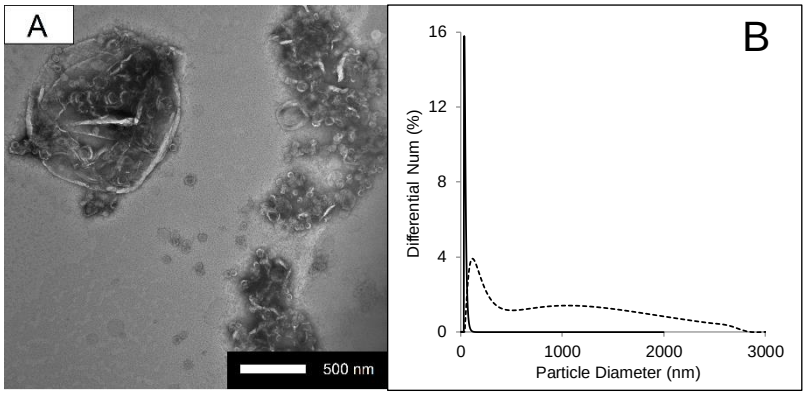

Figure S3.3. (A) TEM image of peptoid-functionalized bicelles prepared in the absence of DTT forming aggregates. peptoid-DHPC = 0.25 mole%. Scale bar represents 500 nm. (B) DLS size distribution curves for non-functionalized (solid) and peptoid-functionalized bicelles with 0.25 mole% in the absence of DTT (dash). q = 1.5

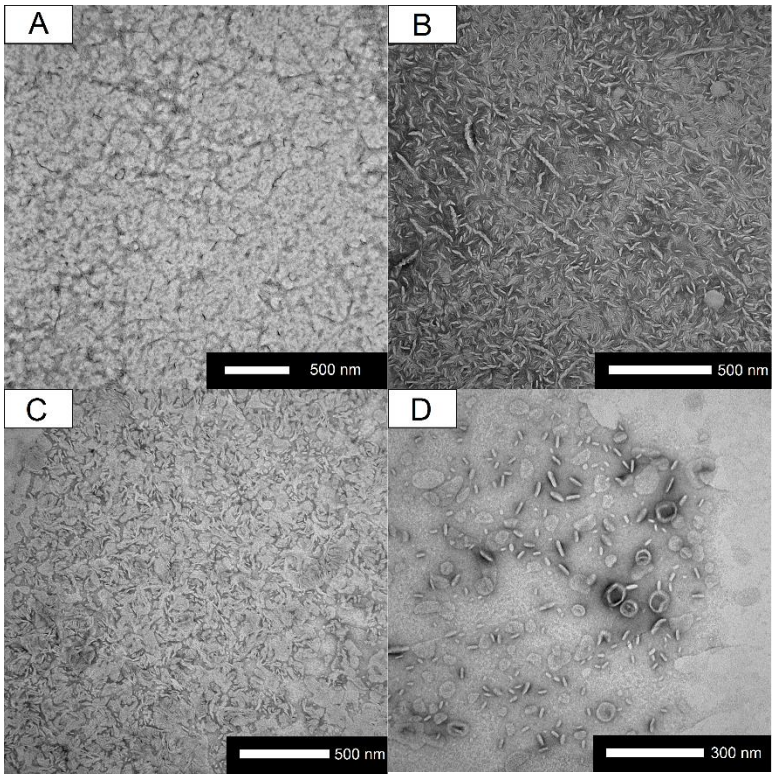

Figure S3.4. Peptoid-functionalized bicelles with different final lipid concentrations by dilution with nanopure water. (A) 6.36, (B) 3.18, (C) 0.318, and (D) 0.159 mM. q = 1.5, peptoid-DHPC = 0.25 mole%. Scale bar represents 500 nm (A, B, C) or 300 nm (D).

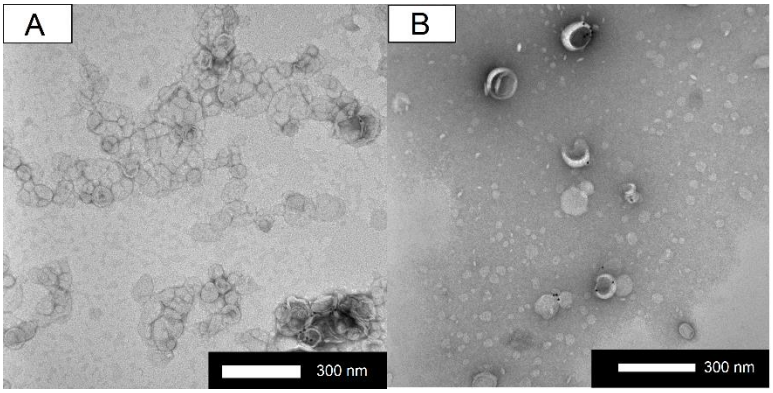

Figure S3.5. TEM images of AuNP modified with (A) non-functionalized bicelles and (B) peptoid-functionalized bicelles with peptoid-DHPC = 0.25 mole% and q=1.5. Scale bar represents 300 nm

Chapter 4 Rational Design of Peptoids to Preferentially Insert into Edge or Plane of Bicelles

4.1. Introduction

Biological membranes play a crucial role in living organisms as major building blocks of cell walls, mitochondria and numerous other cell organelles. They provide stable and functional compartments, control transport, host a number of metabolic and biosynthetic activities, dominate cell-to-cell recognition, and more. Biological membrane have a dynamic nature and complex composition that mainly contains of three types of lipids - the phospholipids, cholesterol and glycolipids- and proteins [94, 130-133].

Phospholipids are one of the most abundant types of lipids in biological membranes that has a hydrophilic head group and a hydrophobic tail. They form a lipid bilayer structure in the aqueous environment, which is energetically (free energy) most favorable. Due to the complexity of biological membranes, it is often required to use a simplified system to model biomembrane structures. These model membrane systems are usually composed of one or two lipids and may have embedded natural proteins, sterols, or artificial peptides. Investigating model cell membranes leads to better understanding of biological membranes functions, lipid-lipid interactions, and drug discovery and delivery [45, 100, 132]. The major classes of model cell membranes are: vesicles [3, 9, 95, 96], supported lipid bilayers [97-99], nanodiscs [37, 38, 100, 101], and bicelles [40, 42, 43, 45, 102, 103].

Vesicles are self-assembled, spherical phospholipid bilayers that closely resembles living cells and can encapsulate materials such as DNA, proteins, drugs, or other chemicals. While vesicles can be relatively easily prepared, they have low stability and the ability of incorporated proteins

to interact with each other is limited [7, 9]. Supported bilayer bilayers (SLBs) are another class of model membrane system where a lipid bilayer is placed on a solid support such as mica, glass or silicon. Several methods have been used to form SLBs including vesicle fusion, the lipid-detergent method, and Langmuir-Blodgett (LB) deposition. SLBs are stable and easy to prepare, while solid surface may affect the membrane protein mobility and function [25, 27, 105].

Both vesicles and SLBs are only accessible from one side, which is a disadvantage; therefore another class of model membrane systems have been developed that are accessible from both sides such as bicelles and nanodiscs. Nanodiscs consist of a segment of phospholipid bilayer surrounded by a membrane scaffold protein (MSP) coat. While nanodiscs have advantages such as monodispersity, access to both sides of the membrane and high stability, they are not applicable in the study of stoichiometric inclusion of multi-protein complexes due to small uniform size range (8 to 13 nm) [35, 36, 38, 106].

Bicelles are nano-disc shape structures composed of long chain lipids (12-18 carbons) and short chain lipids (6–8 carbons). The long and short chain lipids mainly distributed in the plane and edge of the disc, respectively. Bicelles are similar to biological membranes in terms of lipid composition and their planar surface, and they maintain the structure and function of incorporated proteins. The size of bicelles can be varied (10-100nm) which resolves the disadvantage of nanodiscs [39-41, 43].

We previously showed in Chapter 3 that the designed peptoid sequence HN1 is preferentially incorporated into the edges of bicelles. The focus of this part of study is to modify the planar region of bicelles with another designed peptoid sequence peptoid HN2 and investigate the effect

of q and peptoid concentration on morphology and size of peptoid-functionalized bicelles. Peptoid-functionalized bicelles can be used in biosensors by binding to gold nanoring arrays. Moreover, peptoid-functionalized bicelles is applicable as a new media in capillary electrophoresis for membrane protein separation.

Peptoids are a novel class of peptidomimetics that have a backbone similar to peptides with the side chains attached to the amide nitrogen rather than the alpha-carbon. Peptoids were chosen for this application since a large diversity of side chains are available, and they are sequence-specific, easy to synthesize and, resistant to proteolytic degradation [59]. When chiral, aromatic side chains are included, peptoids adopt a polyproline type-I like helix exhibiting a helical pitch of ~6 Å and 3 monomers per turn [62].

Here, for the first time we report the functionalization of planar region of bicelle with peptoid HN2 and evaluate the effect of q and concentration of peptoid HN1 and HN2 on morphology and size of peptoid-functionalized bicelles. The results show that peptoid HN2 preferentially incorporates into the face of the bicelles.

4.2. Materials and Methods

4.2.1. Materials

1,2-dimyristoyl-sn-glycero-3-phosphocholine (DMPC; 14:0 PC) and 1,2-dihexanoyl-sn-glycero-3-phosphocholine (DHPC; 6:0 PC) dissolved in chloroform were purchased from Avanti Polar Lipids (Alabaster, AL). MBHA rink amide resin was purchased from NovaBiochem (Gibbstown, NJ), piperidine was purchased from Sigma-Aldrich (St. Louis, MO), hexylamine, tetradecylamine and S-methylbenzylamine were purchased from Acros Organics (Pittsburgh,

PA) and tert-butyl N-(4-aminobutyl)carbamate was purchased from CNH Technologies Inc. (Woburn, MA). Gold nanoparticles (AuNP) in aqueous solution were purchased from NNCrystal (Fayetteville, AR), and carbon-coated copper grids 300 mesh TYPE A and carbon-coated nickel grids 300 mesh were purchased from Ted Pella. Inc. (Redding, CA). All other reagents and materials were purchased from VWR. All chemicals were used without further modification, unless otherwise noted.

4.2.2. Synthesis of 2-tritysulfanyl-ethylamine

The protected thiol side chain, 2-tritysulfanyl-ethylamine, was prepared as previously described [79]. Briefly, triphenylmethanol was added to the solution of 2-aminoethanethiol hydrochloride in trifluoroacetic acid (TFA). Following incubation, the TFA was removed under reduced pressure using a rotating evaporator (Heidolph Laborota 4001, Elk Grove Village, IL). The solution was triturated with ethyl ether, the precipitant was partitioned with an aqueous solution of NaOH, and the product was extracted with ethyl acetate. The desired product was confirmed by ^{1}H NMR spectroscopy using a Bruker Avance 300 MHz spectrometer (Billerica, MA) equipped with a 5mm BBO probe and compared to previously published data (Supporting information, Figure 2.1) [80].

4.2.3. Peptoid Synthesis and Purification

Peptoids were synthesized *via* a submonomber solid-phase method using an Applied Biosystems 433A automated peptide synthesizer (Carlsband, CA) that was refurbished from a 431A synthesizer [59]. Rink amide resin was swelled with dimethylformamide (DMF) and the Fmoc protecting group was removed using a 20% solution of piperidine in DMF. Then the two-step

submonomer cycle starts with bromoacetylation step by addition of 1.2 M bromoacetic acid in DMF and N, N'-diisopropylcarboniimide at a ratio of 4.3:1. In the next step, side chain amines were added to the resin *via* an SN2 reaction mechanism which consists of incubation with 0.5-1 M amine in DMF for 90 min. The submonomer cycle was repeated until the desired sequence was synthesized. The peptoid was removed from the resin by bathing it in a solution consisting of 95% trifluoroacetic acid (TFA), 2.5% triisoproylsilane, and 2.5% water for 10 min. The acid was removed using a Heidolph Laborota 4001 rotating evaporator (Elk Grove Village, IL) and the product was diluted to a concentration of ~3 mg/mL in a 50:50 solution of isopropanol-water. Peptoids were purified using a preparative reversed-phase high pressure liquid chromatography (RP-HPLC; Waters Delta 600, Milford, MA) with a Duragel G C4 150 x 20 mm column (Peeke Scientific, Novato, CA). Gradients were run at ~1% per min with 30-70% solvent B in A (solvent A: water, 5% isopropanol, 0.1% TFA; solvent B: isopropanol, 5% water, 0.1% TFA) at room temperature (Figure 4.1). Matrix-assisted laser desorption/ionization time of flight (MALDI-TOF) mass spectrometry (Bruker Daltonik GMBH, Bremen, Germany) was used to

confirm that the purified peptoid molecular weight matched the theoretical mass calculated with ChemSketch (ACD/Labs, Toronto, ON). (Figure 4.2)

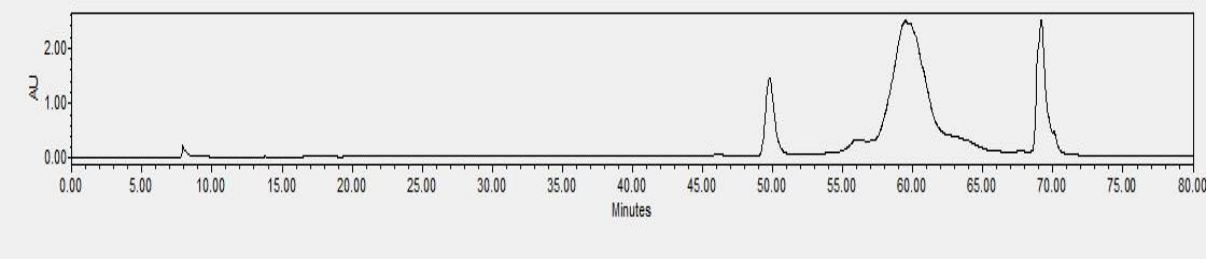

Figure 4.1. RP-HPLC chromatogram of Peptoid HN2

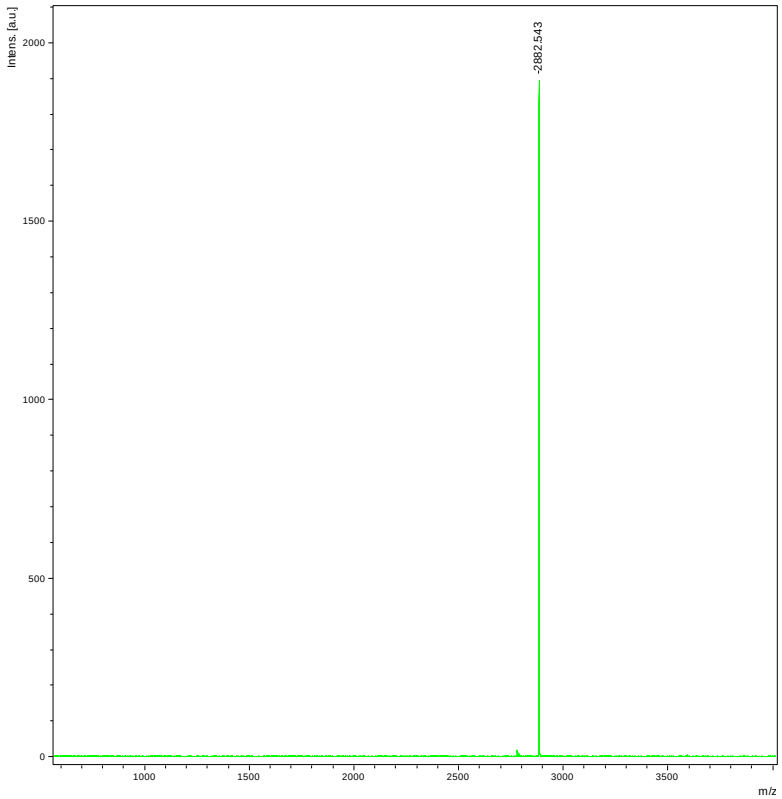

Figure 4.2. MALDI-TOF mass spectrometry was used to confirm that the purified peptoid mas matched the theoretical mass. Mw : 2882 Da.

4.2.4. Circular Dichroism

Circular dichroism (CD) spectroscopy was used to determine the secondary structure of HN1 and HN2. The CD spectra for both peptoids in methanol exhibited a maxima near 190 nm and two minima near 205 and 220 nm [65, 66, 81] (Figure 4.3). CD was performed using a Jasco J-1500 instrument (Easton, MD) at room temperature with a scanning speed of 50 nm/min and a path length of 0.2 mm. The peptoids were dissolved in pure methanol at a concentration of 430 μM and the CD spectra is the cumulative average of 10 scans.

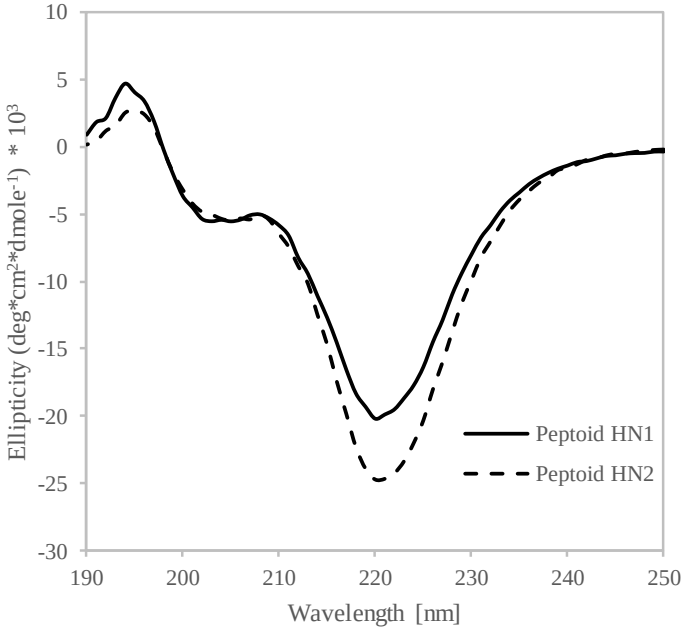

Figure 4.3. Circular dichroism spectra of peptoids HN1 and HN2 showing poly-proline type-1-like helical secondary structure. CD spectra were taken at room temperature with scanning speed of 20 nm/min and a path length of 0.1 mm. The peptoids were dissolved in methanol at a concentration of 430 μM.

4.2.5. Bicelle and Peptoid-functionalized Bicelles Preparation

Bicelles were prepared as previously described [82]. First, chloroform was evaporated from the lipids using a gentle stream of nitrogen gas to form a lipid film, and the samples were then placed under hard vacuum for 12 hr to assure there is no solvent remained. The long-chain lipid was incubated at room temperature for an additional 8 hr before hydration overnight with nanopure water to a final concentration of 0.38 mmole/mL. Then, in order to form liposomes, the hydrated long-chain lipid was incubated at 40 °C for 10 min, vortexed briefly, and placed in an 18 °C ice bath. This cycle was repeated ~3 times, until the solution was free-flowing when heated. The short-chain lipid was hydrated with nanopure water to a final concentration of 0.25 mmole/mL and vortexed at room temperature for 30 sec to form micelles. The desired molar ratio of long-chain (DMPC) to short-chain (DHPC) lipid, referred to as q [40], was mixed together. The lipid mixture (0.63 mmole/mL) was placed on ice for 5 min and vortexed for 1 min. The final step which is the bicelle formation consists of freezing using liquid nitrogen, and thawing in a 45 °C water bath. The freeze-thaw cycle was repeated ~10 times until the solution was transparent after being placed on ice for 5 min.

Peptoid-functionalized bicelles were prepared by peptoid addition before bicelle formation (Method 2 in Chapter 3). In order to prevent the formation of disulfide bonds, The reducing agent DTT was added to the peptoid solution at 1 mM prior to adding to the bicelle solution [83]. The amount of q for peptoid-functionalized bicelles was defined based on the aimed modification region:

$$q = \frac{mole\ DMPC}{mole\ (DHPC+peptoid\ HN1)}$$ Edge modification (Equation 4.1)

$$q = \frac{mole\ (DMPC+peptoid\ HN2)}{mole\ DHPC}$$ Planar modification (Equation 4.2)

4.2.6. Transmission Electron Microscopy

Transmission Electron Microscopy (TEM) was used to visualized bicelles and peptoid-functionalized bicelles as previously described [42, 45, 84, 85]. TEM grids were prepared by dropping 5 µL of diluted bicelle solution onto a 300 square mesh formvar-carbon supported copper at room temperature. The grids were placed on filter paper to dry, stained with 2% uranyl acetate, and placed on filter paper to dry overnight. Images were obtained using a JEOL-1011 TEM (Tokyo, Japan) with an accelerating voltage of 110 kV. Microsoft Visio was used to determine the diameter and thickness of the bicelles from the TEM images. In order to obtain clear TEM images of the bicelles, samples were diluted with nanopure water [86].

4.2.7. Determination of Peptoid Position

The location of peptoids within the bicelles was determined by incubation with AuNP. The AuNP size is 10±2 nm and the AuNP solution concentration is 40-50 µg/mL. 1.5 µL of non-functionalized and peptoid-functionalized bicelle solutions were combined with 1.0 mL of AuNP solution in 1.5 mL nanopure water [87] and incubated for 1 hr on an orbital vortexer to allow for AuNP attachment to the thiols at the N-terminus of peptoid HN1 [88-91]. AuNP-peptoid-functionalized bicelles were visualized by TEM without any further dilution, as described above.

4.3. Results

4.3.1. Peptoids Sequence and Rational

The design of peptoids sequence is based on work in the Barron lab that showed that alkylation of a cationic, facially amphipathic peptoid led to improved insertion into lipid films [114]. Both peptoids reported here have three functional regions (Figure 4.4): (1) insertion sequence, (2) facially amphipathic helix (charged anchor), and (3) functional groups. The insertion region is includes two alkyl chains and two hydrophobic, chiral aromatic groups. The length of alkyl chains depends on the target region of bicelle that needs to be modified which is the length of the DHPC tail groups that make up the bicelle edge (6 carbons) for edge modification or the length of DMPC tail groups that make up the bicelle face (14 carbons) for planar modification. This region of the peptoid serves as an anchor into the bicelle edge or face and inserts into the hydrophobic lipid tail region. To induce helical secondary structure, the facially amphipathic helix contains chiral aromatic groups with three residues per turn [62]. One side of the helix is hydrophobic to interact with the lipid tails, and the other side contains positive charges to interact

with the lipid head groups. In order to determine peptoid location within the bicelle, thiol was selected as the functional group to use for AuNP attachment studies.

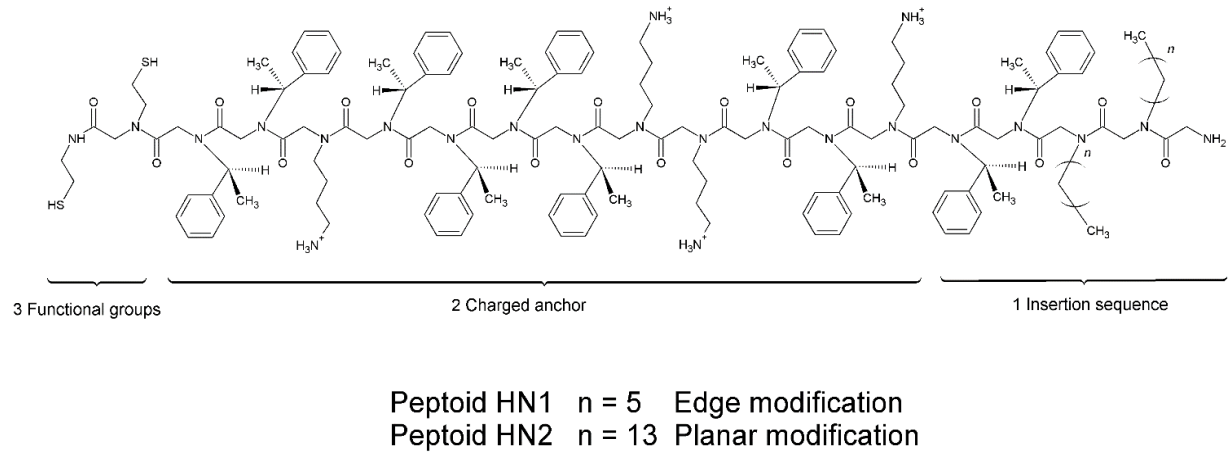

Figure 4.4. Peptoids HN1 and HN2 structure. There are 3 active regions on the peptoids: (1) insertion sequence, (2) charged anchor, and (3) functional groups.

4.3.2. Placement of Peptoids within Bicelles

The position of peptoids within the bicelle was evaluated using AuNP attachment to the thiol groups at the N-terminus of peptoids. Then, AuNP-peptoid-functionalized bicelles were visualized by TEM. For edge modification, previous studies in Chapter 3 showed that peptoid position in the bicelle were completed at 20 mole% peptoid HN1 with 82% peptoid incorporation into the bicelle edge (Figure 4.5A). TEM images of AuNP-peptoid-functionalized bicelles using peptoid HN2 for planar modification showed that peptoid incorporated preferentially into the faces of bicelle at 40 mole% peptoid. (Figure 4.5B). TEM image analysis showed 92% peptoid incorporation into the bicelle face, as opposed to the edge.

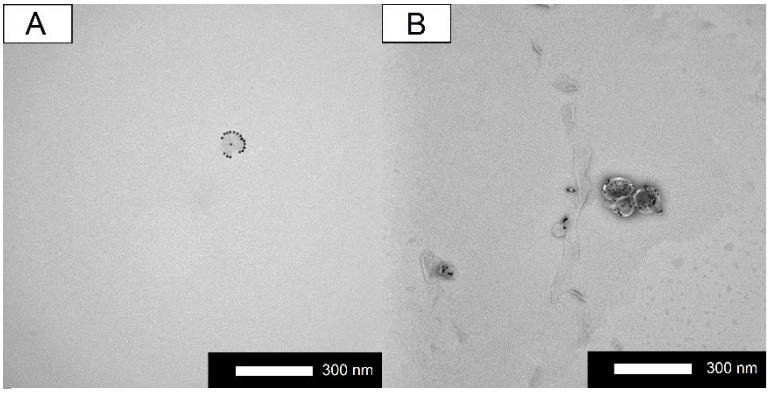

Figure 4.5. TEM images of AuNP modified peptoid-functionalized bicelles with (A) Peptoid HN1, peptoid-DHPC = 20 mole% and (B) Peptoid HN2, peptoid-DMPC = 40 mole% . q=1.5

4.3.3. Morphology Studies of Bicelles and Peptoid-functionalized Bicelles

Bicelles and peptoid-functionalized bicelles (composed of DMPC and DHPC) at different levels of q, and peptoid concentration using both peptoid HN1 and HN2 were prepared and morphology and size were investigated by TEM imaging. Bicelle samples were prepared after 100-fold dilution. TEM images showed that at all levels of q, bicelles were observed mostly in edge-on projections which is due to the high concentration of bicelles in the sample (Figure 4.6). The average diameter for bicelles was 31.6±13.0 nm, 36.5±13.0 nm, 47.3±17.8 nm for q=0.5, 1.5, and 3.2 respectively, in accordance with previously published data for DMPC:DHPC bicelles [41, 123-125].

Morphology studies for peptoid HN1 and HN2 are shown in Figure 4.7 and Figure 4.8, respectively. TEM images showed that peptoid-functionalized bicelles had similar morphology to bicelles and addition of peptoid did not alter the structure of bicelles. For each value of q,

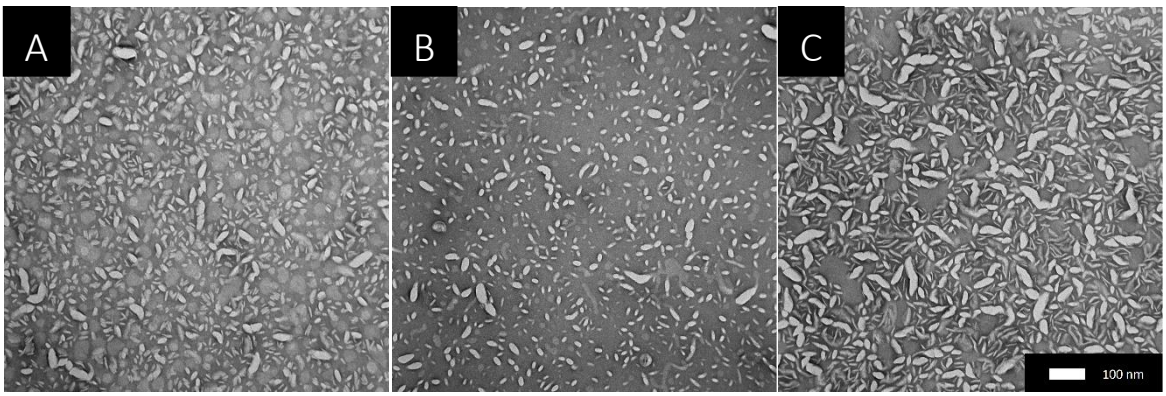

Figure 4.6. TEM images of DMPC/DHPC bicelles at different q levels. (A) q=0.5, (B) q=1.5, (C) q=3.2. Scale bar represents 100 nm.

peptoid-functionalized bicelles with different peptoid concentration had similar size to bicelles.

The average diameter for bicelles and peptoid-functionalized bicelles is presented in Table 4.1.

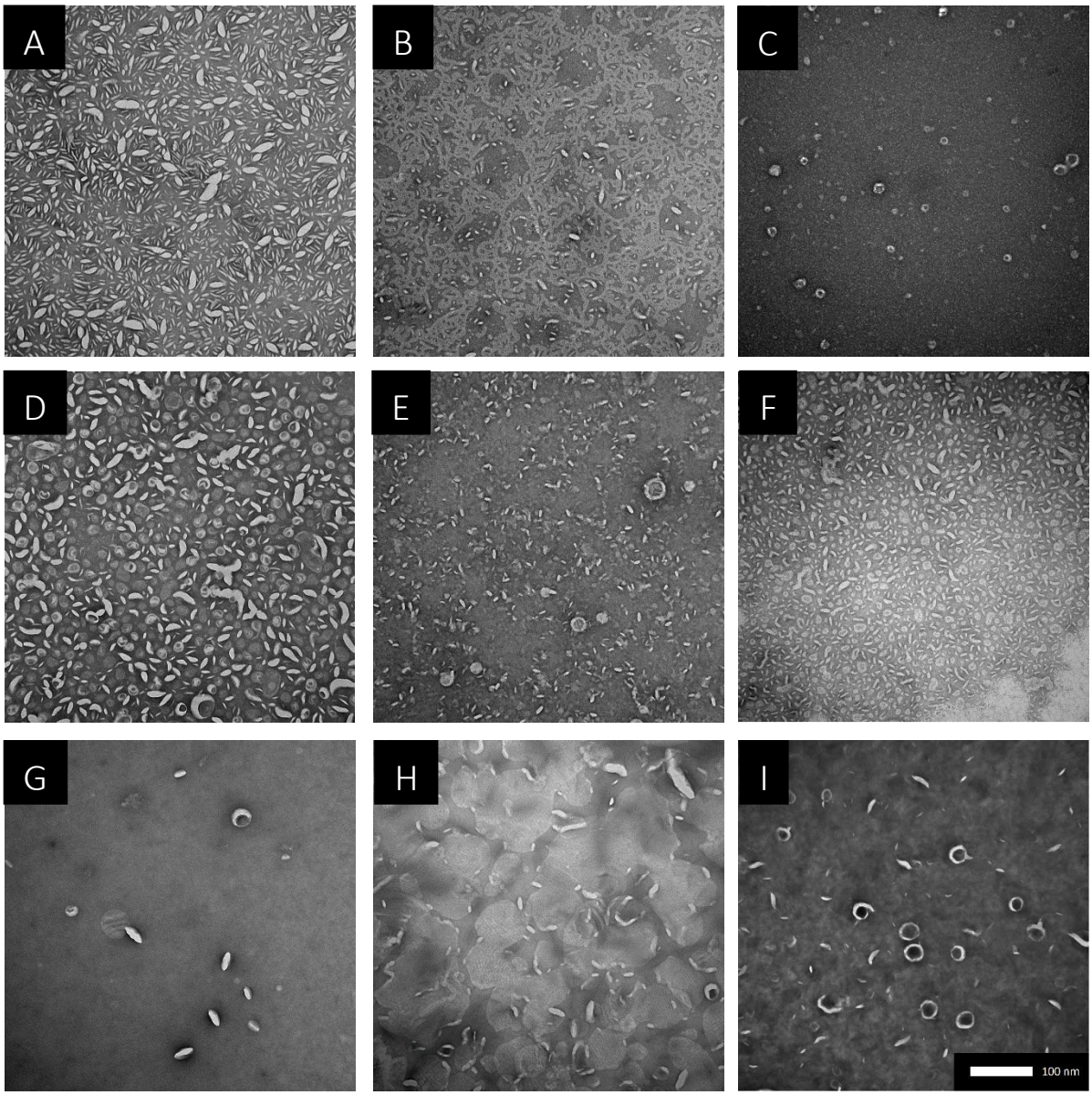

Figure 4.7. TEM images of peptoid-functionalized bicelles with peptoid HN1. q = 0.5: (A) peptoid-DHPC = 0.25 mole%, (B) peptoid-DHPC = 2.5 mole%, (C) = peptoid-DHPC = 5 mole%. q = 1.5: (D) peptoid-DHPC = 0.25 mole%, (E) peptoid-DHPC = 2.5 mole%, (F) = peptoid-DHPC = 5 mole%. q = 3.2: (G) peptoid-DHPC = 0.25 mole%, (H) peptoid-DHPC = 2.5 mole%, (I) = peptoid-DHPC = 5 mole%.Scale bar represents 100 nm.

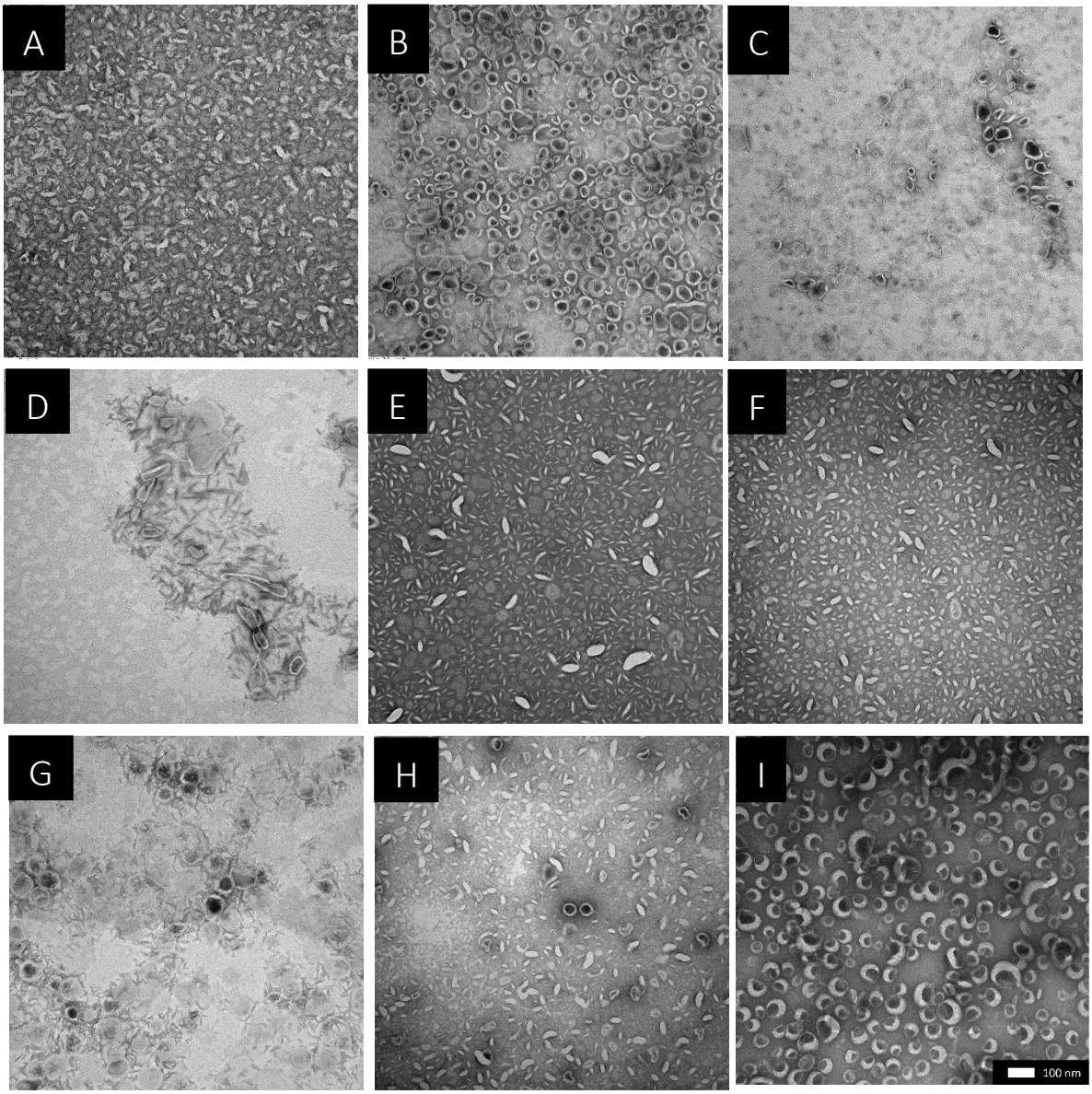

Figure 4.8. TEM images of peptoid-functionalized bicelles with peptoid HN2. q = 0.5: (A) peptoid-DMPC = 0.25 mole%, (B) peptoid-DMPC = 2.5 mole%, (C) = peptoid-DMPC = 5 mole%. q = 1.5: (D) peptoid-DMPC = 0.25 mole%, (E) peptoid-DMPC = 2.5 mole%, (F) = peptoid-DMPC = 5 mole%. q = 3.2: (G) peptoid-DMPC = 0.25 mole%, (H) peptoid-DMPC = 2.5 mole%, (I) = peptoid-DMPC = 5 mole%. Scale bar represents 100 nm.

4.4. Conclusion

Here, for the first time, we report the formation of peptoid-functionalized bicelles with peptoid preferentially at the faces. The insertion region of peptoid which contains alkyl chain matching the length of the DMPC tail groups, preferentially assembled with the DMPC at the faces of bicelle. Preferential incorporation of the peptoid into the bicelle edge was confirmed by attachment of AuNPs to the thiol groups on the N-terminus of the peptoid. Peptoid-functionalized bicelles showed preferential placement in the bicelle edge (~92%). The insertion of peptoid in the edge region of bicelle is unlikely, since the alkyl chain length of peptoid is longer than the length of the DHPC tail groups.

The increase in the size of bicelle with higher q is predictable as q is the ratio of molecules that forms faces of bicelles to the molecules that forms edges. Moreover, morphology studies of peptoid-functionalized bicelles using both peptoid HN1 and peptoid HN2 at different levels of q and peptoid concentration show that addition of peptoid doesn't change the structure of bicelles. For each level of q, addition of peptoid doesn't change the size of bicelles which is due to the small size of peptoid (~30 A°).

Table 4.1. Size analysis of peptoid-functionalized at different levels of q and peptoid concentrations using peptoids HN1 and HN2

Peptoid/lipid %	**Peptoid-functionalized bicelles diameter (nm)**						
	0		0.25		2.5	5	
Modification	___	Edge	Face	Edge	Face	Edge	Face
q = 0.5	31.6±13.0	33.5±12.0	31.2±10.3	32.6±12.7	35.8±12.6	32.4±15.3	34.1±16.2
q = 1.5	36.5±13.0	47.8±14.3	39.7±18.0	43.0±17.2	38.2±16.9	42.2±16.0	37.4±13.1
q = 3.2	47.3±17.8	45.1±18.9	57.6±19.3	42.7±13.2	57.0±15.4	43.0±12.6	62.6±18.4

4.5. Future Work

Future studies can be continued in several directions. The stability of peptoid-functionalized bicelles may be determined and compared to bicelles using NMR. Moreover, peptoid-functionalized bicelles can be formed using different lipids including saturated and unsaturated and then incorporation of peptoid HN1 and HN2 into the bicelle structure may be investigated.

Furthermore, peptoid-functionalized bicelles have great potential to use as drug carriers for tumor targeted drug delivery. Therefore, membrane proteins can be incorporated into peptoid-functiolized bicelles using other functional groups in peptoid HN1 sequence instead of thiol for edge modification in order to form nanocarriers and compare the results with lipodisks.

References

1. Pereira-Leite, C., C. Nunes, and S. Reis, *Interaction of nonsteroidal anti-inflammatory drugs with membranes: in vitro assessment and relevance for their biological actions.* Progress in lipid research, 2013. **52**(4): p. 571-584.

2. Shi, Y., et al., *The structure and function of cell membranes studied by atomic force microscopy.* Seminars in Cell & Developmental Biology, 2017.

3. Edidin, M., *The state of lipid rafts: from model membranes to cells.* Annual review of biophysics and biomolecular structure, 2003. **32**(1): p. 257-283.

4. Pomorski, T.G., T. Nylander, and M. Cárdenas, *Model cell membranes: discerning lipid and protein contributions in shaping the cell.* Advances in colloid and interface science, 2014. **205**: p. 207-220.

5. Singer, S.J. and G.L. Nicolson, *The fluid mosaic model of the structure of cell membranes.* Science, 1972. **175**(4023): p. 720-731.

6. Goñi, F.M., *The basic structure and dynamics of cell membranes: An update of the Singer–Nicolson model.* Biochimica et Biophysica Acta (BBA) - Biomembranes, 2014. **1838**(6): p. 1467-1476.

7. Chan, Y.-H.M. and S.G. Boxer, *Model membrane systems and their applications.* Current opinion in chemical biology, 2007. **11**(6): p. 581-587.

8. Czogalla, A., et al., *Validity and applicability of membrane model systems for studying interactions of peripheral membrane proteins with lipids.* Biochimica et Biophysica Acta (BBA)-Molecular and Cell Biology of Lipids, 2014. **1841**(8): p. 1049-1059.

9. Peetla, C., A. Stine, and V. Labhasetwar, *Biophysical interactions with model lipid membranes: applications in drug discovery and drug delivery.* Molecular pharmaceutics, 2009. **6**(5): p. 1264-1276.

10. Pollock, N.L., et al., *Structure and function of membrane proteins encapsulated in a polymer-bound lipid bilayer.* Biochimica et Biophysica Acta (BBA)-Biomembranes, 2017.

11. Almeida, J.G., et al., *Membrane proteins structures: A review on computational modeling tools.* Biochimica et Biophysica Acta (BBA) - Biomembranes, 2017. **1859**(10): p. 2021-2039.

12. van Swaay, D., *Microfluidic methods for forming liposomes.* Lab on a Chip, 2013. **13**(5): p. 752-767.

13. Rendi, R., *Water extrusion in isolated subcellular fractions VI. Osmostic properties of swollen phospholipid suspensions.* Biochimica et Biophysica Acta (BBA)-Biomembranes, 1967. **135**(2): p. 333-346.

14. Papahadjopoulos, D. and J. Watkins, *Phospholipid model membranes. II. Permeability properties of hydrated liquid crystals.* Biochimica et Biophysica Acta (BBA)-Biomembranes, 1967. **135**(4): p. 639-652.

15. Šegota, S., *Spontaneous formation of vesicles.* Advances in colloid and interface science, 2006. **121**(1): p. 51-75.

16. Angelova, M.I. and D.S. Dimitrov, *Liposome electroformation.* Faraday discussions of the Chemical Society, 1986. **81**: p. 303-311.

17. Wang, T., et al., *Preparation of submicron unilamellar liposomes by freeze-drying double emulsions.* Biochimica et Biophysica Acta (BBA)-Biomembranes, 2006. **1758**(2): p. 222-231.

18. Long, M.S., A.-S. Cans, and C.D. Keating, *Budding and asymmetric protein microcompartmentation in giant vesicles containing two aqueous phases.* Journal of the American Chemical Society, 2008. **130**(2): p. 756-762.

19. Akbarzadeh, A., et al., *Liposome: classification, preparation, and applications.* Nanoscale research letters, 2013. **8**(1): p. 102.

20. Szoka Jr, F. and D. Papahadjopoulos, *Comparative properties and methods of preparation of lipid vesicles (liposomes).* Annual review of biophysics and bioengineering, 1980. **9**(1): p. 467-508.

21. Rieth, M.D., *Investigating Detergent and Lipid Systems for the Study of Membrane Protein Interactions: Characterizing Caveolin Oligomerization*. 2014, LEHIGH UNIVERSITY.

22. Seddon, A.M., P. Curnow, and P.J. Booth, *Membrane proteins, lipids and detergents: not just a soap opera.* Biochimica et Biophysica Acta (BBA) - Biomembranes, 2004. **1666**(1–2): p. 105-117.

23. Shen, H.-H., T. Lithgow, and L. Martin, *Reconstitution of membrane proteins into model membranes: seeking better ways to retain protein activities.* International journal of molecular sciences, 2013. **14**(1): p. 1589-1607.

24. Brian, A.A. and H.M. McConnell, *Allogeneic stimulation of cytotoxic T cells by supported planar membranes.* Proceedings of the National Academy of Sciences, 1984. **81**(19): p. 6159-6163.

25. Castellana, E.T. and P.S. Cremer, *Solid supported lipid bilayers: From biophysical studies to sensor design.* Surface Science Reports, 2006. **61**(10): p. 429-444.

26. Tamm, L.K. and H.M. McConnell, *Supported phospholipid bilayers.* Biophysical Journal, 1985. **47**(1): p. 105-113.

27. Sackmann, E., *Supported membranes: scientific and practical applications.* Science-AAAS-Weekly Paper Edition, 1996. **271**(5245): p. 43-48.

28. Cremer, P.S. and S.G. Boxer, *Formation and spreading of lipid bilayers on planar glass supports.* The Journal of Physical Chemistry B, 1999. **103**(13): p. 2554-2559.

29. Stelzle, M., R. Miehlich, and E. Sackmann, *Two-dimensional microelectrophoresis in supported lipid bilayers.* Biophysical journal, 1992. **63**(5): p. 1346-1354.

30. Holden, M.A., et al., *Creating fluid and air-stable solid supported lipid bilayers.* Journal of the American Chemical Society, 2004. **126**(21): p. 6512-6513.

31. Plant, A.L., *Supported hybrid bilayer membranes as rugged cell membrane mimics.* Langmuir, 1999. **15**(15): p. 5128-5135.

32. Ross, E.E., et al., *Planar supported lipid bilayer polymers formed by vesicle fusion. 1. Influence of diene monomer structure and polymerization method on film properties.* Langmuir, 2003. **19**(5): p. 1752-1765.

33. Conboy, J.C., et al., *Planar Supported Bilayer Polymers Formed from Bis-Diene Lipids by Langmuir− Blodgett Deposition and UV Irradiation.* Biomacromolecules, 2003. **4**(3): p. 841-849.

34. Morigaki, K., K. Kiyosue, and T. Taguchi, *Micropatterned composite membranes of polymerized and fluid lipid bilayers.* Langmuir, 2004. **20**(18): p. 7729-7735.

35. Goluch, E.D., et al., *Microfluidic patterning of nanodisc lipid bilayers and multiplexed analysis of protein interaction.* Lab on a Chip, 2008. **8**(10): p. 1723-1728.

36. Bayburt, T.H. and S.G. Sligar, *Membrane protein assembly into Nanodiscs.* FEBS letters, 2010. **584**(9): p. 1721-1727.

37. Ritchie, T., et al., *Chapter eleven-reconstitution of membrane proteins in phospholipid bilayer nanodiscs.* Methods in enzymology, 2009. **464**: p. 211-231.

38. Nath, A., W.M. Atkins, and S.G. Sligar, *Applications of phospholipid bilayer nanodiscs in the study of membranes and membrane proteins.* Biochemistry, 2007. **46**(8): p. 2059-2069.

39. Beaugrand, M., et al., *Lipid Concentration and Molar Ratio Boundaries for the Use of Isotropic Bicelles.* Langmuir, 2014.

40. Dürr, U.H., M. Gildenberg, and A. Ramamoorthy, *The magic of bicelles lights up membrane protein structure.* Chemical reviews, 2012. **112**(11): p. 6054-6074.

41. Matsumori, N. and M. Murata, *3D structures of membrane-associated small molecules as determined in isotropic bicelles.* Natural product reports, 2010. **27**(10): p. 1480-1492.

42. Diller, A., et al., *Bicelles: a natural 'molecular goniometer'for structural, dynamical and topological studies of molecules in membranes.* Biochimie, 2009. **91**(6): p. 744-751.

43. Sanders, C.R. and R.S. Prosser, *Bicelles: a model membrane system for all seasons?* Structure, 1998. **6**(10): p. 1227-1234.

44. Sternin, E., D. Nizza, and K. Gawrisch, *Temperature dependence of DMPC/DHPC mixing in a bicellar solution and its structural implications.* Langmuir, 2001. **17**(9): p. 2610-2616.

45. Glover, K.J., et al., *Structural evaluation of phospholipid bicelles for solution-state studies of membrane-associated biomolecules.* Biophysical journal, 2001. **81**(4): p. 2163-2171.

46. Marcotte, I. and M. Auger, *Bicelles as model membranes for solid-and solution-state NMR studies of membrane peptides and proteins.* Concepts in Magnetic Resonance Part A, 2005. **24**(1): p. 17-37.

47. Dürr, U.H., R. Soong, and A. Ramamoorthy, *When detergent meets bilayer: birth and coming of age of lipid bicelles.* Progress in nuclear magnetic resonance spectroscopy, 2013. **69**: p. 1.

48. Warschawski, D.E., et al., *Choosing membrane mimetics for NMR structural studies of transmembrane proteins.* Biochimica et Biophysica Acta (BBA)-Biomembranes, 2011. **1808**(8): p. 1957-1974.

49. Faham, S., et al., *Practical aspects of membrane proteins crystallization in bicelles.* Current topics in membranes, 2009. **63**: p. 109-125.

50. Naito, A., *Structure elucidation of membrane-associated peptides and proteins in oriented bilayers by solid-state NMR spectroscopy.* Solid state nuclear magnetic resonance, 2009. **36**(2): p. 67-76.

51. Ram, P. and J. Prestegard, *Magnetic field induced ordering of bile salt/phospholipid micelles: new media for NMR structural investigations.* Biochimica et Biophysica Acta (BBA)-Biomembranes, 1988. **940**(2): p. 289-294.

52. Triba, M.N., D.E. Warschawski, and P.F. Devaux, *Reinvestigation by phosphorus NMR of lipid distribution in bicelles.* Biophysical journal, 2005. **88**(3): p. 1887-1901.

53. Sanders, C.R. and G.C. Landis, *Facile acquisition and assignment of oriented sample NMR spectra for bilayer surface-associated proteins.* Journal of the American Chemical Society, 1994. **116**(14): p. 6470-6471.

54. Ottiger, M. and A. Bax, *Characterization of magnetically oriented phospholipid micelles for measurement of dipolar couplings in macromolecules.* Journal of biomolecular NMR, 1998. **12**(3): p. 361-372.

55. Yamamoto, K., R. Soong, and A. Ramamoorthy, *Comprehensive analysis of lipid dynamics variation with lipid composition and hydration of bicelles using nuclear magnetic resonance (NMR) spectroscopy.* Langmuir, 2009. **25**(12): p. 7010-7018.

56. Son, W.S., et al., *'q-Titration'of long-chain and short-chain lipids differentiates between structured and mobile residues of membrane proteins studied in bicelles by solution NMR spectroscopy.* Journal of magnetic resonance, 2012. **214**: p. 111-118.

57. Miller, S.M., et al., *Comparison of the proteolytic susceptibilities of homologous L-amino acid, D-amino acid, and N-substituted glycine peptide and peptoid oligomers.* Drug Development Research, 1995. **35**(1): p. 20-32.

58. Simon, R.J., et al., *Peptoids: a modular approach to drug discovery.* Proceedings of the National Academy of Sciences, 1992. **89**(20): p. 9367-9371.

59. Zuckermann, R.N., et al., *Efficient method for the preparation of peptoids [oligo (N-substituted glycines)] by submonomer solid-phase synthesis.* Journal of the American Chemical Society, 1992. **114**(26): p. 10646-10647.

60. Tran, H., et al., *Solid-phase submonomer synthesis of peptoid polymers and their self-assembly into highly-ordered nanosheets.* Journal of visualized experiments: JoVE, 2011(57).

61. Armand, P., et al., *Chiral N-substituted glycines can form stable helical conformations.* Folding and Design, 1997. **2**(6): p. 369-375.

62. Armand, P., et al., *NMR determination of the major solution conformation of a peptoid pentamer with chiral side chains.* Proceedings of the National Academy of Sciences, 1998. **95**(8): p. 4309-4314.

63. Patch, J.A., et al., *Versatile Oligo(N-Substituted) Glycines: The Many Roles of Peptoids in Drug Discovery*, in *Pseudo-Peptides in Drug Development*. 2005, Wiley-VCH Verlag GmbH & Co. KGaA. p. 1-31.

64. Hebert, M.L., et al., *Tunable peptoid microspheres: effects of side chain chemistry and sequence.* Organic & biomolecular chemistry, 2013. **11**(27): p. 4459-4464.

65. Wu, C.W., et al., *Peptoid oligomers with α-chiral, aromatic side chains: sequence requirements for the formation of stable peptoid helices.* Journal of the American Chemical Society, 2001. **123**(28): p. 6778-6784.

66. Wu, C.W., et al., *Peptoid oligomers with α-chiral, aromatic side chains: effects of chain length on secondary structure.* Journal of the American Chemical Society, 2001. **123**(13): p. 2958-2963.

67. Seurynck, S.L., J.A. Patch, and A.E. Barron, *Simple, helical peptoid analogs of lung surfactant protein B.* Chemistry & biology, 2005. **12**(1): p. 77-88.

68. Wu, C.W., et al., *Helical peptoid mimics of lung surfactant protein C.* Chemistry & biology, 2003. **10**(11): p. 1057-1063.

69. Seurynck-Servoss, S.L., M.T. Dohm, and A.E. Barron, *Effects of including an N-terminal insertion region and arginine-mimetic side chains in helical peptoid analogues of lung surfactant protein B.* Biochemistry, 2006. **45**(39): p. 11809-11818.

70. Walther, F.J., et al., *Comparison of three lipid formulations for synthetic surfactant with a surfactant protein B analog.* Experimental lung research, 2005. **31**(6): p. 563-579.

71. Seurynck-Servoss, S.L., et al., *Lipid composition greatly affects the in vitro surface activity of lung surfactant protein mimics.* Colloids and Surfaces B: Biointerfaces, 2007. **57**(1): p. 37-55.

72. Brown, N.J., et al., *Effects of hydrophobic helix length and side chain chemistry on biomimicry in peptoid analogues of SP-C.* Biochemistry, 2008. **47**(6): p. 1808-1818.

73. Chongsiriwatana, N.P., et al., *Peptoids that mimic the structure, function, and mechanism of helical antimicrobial peptides.* Proceedings of the National Academy of Sciences, 2008. **105**(8): p. 2794-2799.

74. Reijmar, K., et al., *Characterizing and Controlling the Loading and Release of Cationic Amphiphilic Peptides onto and from PEG-Stabilized Lipodisks.* Langmuir, 2016. **32**(46): p. 12091-12099.

75. Gao, J., et al., *RGD-modified lipid disks as drug carriers for tumor targeted drug delivery.* Nanoscale, 2016. **8**(13): p. 7209-7216.

76. Ahlgren, S., K. Reijmar, and K. Edwards, *Targeting lipodisks enable selective delivery of anticancer peptides to tumor cells.* Nanomedicine: Nanotechnology, Biology and Medicine, 2017. **13**(7): p. 2325-2328.

77. Veronese, F.M. and G. Pasut, *PEGylation, successful approach to drug delivery.* Drug discovery today, 2005. **10**(21): p. 1451-1458.

78. Lucyanna, B.-B., et al., *Structural versatility of bicellar systems and their possibilities as colloidal carriers.* Pharmaceutics, 2011. **3**(3): p. 636-664.

79. Guo, W., et al., *Luminescent CdSe/CdS Core/Shell Nanocrystals in Dendron Boxes: Superior Chemical, Photochemical and Thermal Stability.* Journal of the American Chemical Society, 2003. **125**(13): p. 3901-3909.

80. Gottlieb, H.E., V. Kotlyar, and A. Nudelman, *NMR chemical shifts of common laboratory solvents as trace impurities.* The Journal of organic chemistry, 1997. **62**(21): p. 7512-7515.

81. Wu, C.W., et al., *Structural and spectroscopic studies of peptoid oligomers with α-chiral aliphatic side chains.* Journal of the American Chemical Society, 2003. **125**(44): p. 13525-13530.

82. De Angelis, A.A. and S.J. Opella, *Bicelle samples for solid-state NMR of membrane proteins.* Nature protocols, 2007. **2**(10): p. 2332-2338.

83. Konigsberg, W., *[13] Reduction of disulfide bonds in proteins with dithiothreitol.* Methods in enzymology, 1972. **25**: p. 185-188.

84. Barbosa-Barros, L., et al., *Morphological effects of ceramide on DMPC/DHPC bicelles.* Journal of microscopy, 2008. **230**(1): p. 16-26.

85. Scholtysek, P., et al., *A T-shaped amphiphilic molecule forms closed vesicles in water and bicelles in mixtures with a membrane lipid.* The Journal of Physical Chemistry B, 2012. **116**(16): p. 4871-4878.

86. Beaugrand, M., et al., *Lipid concentration and molar ratio boundaries for the use of isotropic bicelles.* Langmuir, 2014. **30**(21): p. 6162-6170.

87. Zhong, Z., et al., *The surface chemistry of Au colloids and their interactions with functional amino acids.* The Journal of Physical Chemistry B, 2004. **108**(13): p. 4046-4052.

88. Aryal, S., et al., *Study of electrolyte induced aggregation of gold nanoparticles capped by amino acids.* Journal of colloid and interface science, 2006. **299**(1): p. 191-197.

89. Daniel, M.-C. and D. Astruc, *Gold nanoparticles: assembly, supramolecular chemistry, quantum-size-related properties, and applications toward biology, catalysis, and nanotechnology.* Chemical reviews, 2004. **104**(1): p. 293-346.

90. Li, Z.P., et al., *Selective determination of cysteine by resonance light scattering technique based on self-assembly of gold nanoparticles.* Analytical biochemistry, 2006. **351**(1): p. 18-25.

91. Naka, K., et al., *Effect of Gold Nanoparticles as a Support for the Oligomerization of L-Cysteine in an Aqueous Solution.* Langmuir, 2003. **19**(13): p. 5546-5549.

92. Edwards, K.A. and A.J. Baeumner, *Analysis of liposomes.* Talanta, 2006. **68**(5): p. 1432-1441.

93. Mazer, N.A., G.B. Benedek, and M.C. Carey, *Quasielastic light-scattering studies of aqueous biliary lipid systems. Mixed micelle formation in bile salt-lecithin solutions.* Biochemistry, 1980. **19**(4): p. 601-615.

94. Alberts, B., Johnson, A., Lewis, J., et al., *Membrane Structure: The Lipid Bilayer*, in *Molecular Biology of the Cell*. 2002, Garland Science: New York. p. 583-614.

95. Bangham, A., M. Hill, and N. Miller, *Preparation and use of liposomes as models of biological membranes*. 1974: Springer.

96. Dietrich, C., et al., *Lipid rafts reconstituted in model membranes.* Biophysical journal, 2001. **80**(3): p. 1417-1428.

97. Richter, R.P., R. Bérat, and A.R. Brisson, *Formation of solid-supported lipid bilayers: an integrated view.* Langmuir, 2006. **22**(8): p. 3497-3505.

98. Boxer, S.G., *Molecular transport and organization in supported lipid membranes.* Current opinion in chemical biology, 2000. **4**(6): p. 704-709.

99. Groves, J.T. and S.G. Boxer, *Micropattern formation in supported lipid membranes.* Accounts of Chemical Research, 2002. **35**(3): p. 149-157.

100. Bayburt, T.H., Y.V. Grinkova, and S.G. Sligar, *Self-assembly of discoidal phospholipid bilayer nanoparticles with membrane scaffold proteins.* Nano Letters, 2002. **2**(8): p. 853-856.

101. Hagn, F., et al., *Optimized phospholipid bilayer nanodiscs facilitate high-resolution structure determination of membrane proteins.* Journal of the American Chemical Society, 2013. **135**(5): p. 1919-1925.

102. Vestergaard, M., et al., *Bicelles and Other Membrane Mimics: Comparison of Structure, Properties, and Dynamics from MD Simulations.* The Journal of Physical Chemistry B, 2015. **119**(52): p. 15831-15843.

103. Wu, H., et al., *Assessing the size, stability, and utility of isotropically tumbling bicelle systems for structural biology*. Biochimica et Biophysica Acta (BBA)-Biomembranes, 2010. **1798**(3): p. 482-488.

104. Yamamoto, S., Y. Maruyama, and S.-a. Hyodo, *Dissipative particle dynamics study of spontaneous vesicle formation of amphiphilic molecules.* The Journal of chemical physics, 2002. **116**(13): p. 5842-5849.

105. Richter, R.P., R. Bérat, and A.R. Brisson, *Formation of Solid-Supported Lipid Bilayers: An Integrated View.* Langmuir, 2006. **22**(8): p. 3497-3505.

106. Borch, J. and T. Hamann, *The nanodisc: a novel tool for membrane protein studies.* Biological chemistry, 2009. **390**(8): p. 805-814.

107. Arnold, A., et al., *Cation Modulation of Bicelle Size and Magnetic Alignment as Revealed by Solid-State NMR and Electron Microscopy*. Biophysical Journal, 2002. **83**(5): p. 2667-2680.

108. Johansson, E., et al., *Development and initial evaluation of PEG-stabilized bilayer disks as novel model membranes.* Biophysical chemistry, 2005. **113**(2): p. 183-192.

109. Johansson, E., et al., *Nanosized bilayer disks: Attractive model membranes for drug partition studies.* Biochimica et Biophysica Acta (BBA) - Biomembranes, 2007. **1768**(6): p. 1518-1525.

110. Johnsson, M. and K. Edwards, *Liposomes, disks, and spherical micelles: aggregate structure in mixtures of gel phase phosphatidylcholines and poly (ethylene glycol)-phospholipids.* Biophysical Journal, 2003. **85**(6): p. 3839-3847.

111. Zetterberg, M.M., et al., *Optimization of lipodisk properties by modification of the extent and density of the PEG corona.* Journal of Colloid and Interface Science, 2016. **484**(Supplement C): p. 86-96.

112. Lundquist, A., et al., *Melittin–Lipid interaction: A comparative study using liposomes, micelles and bilayerdisks.* Biochimica et Biophysica Acta (BBA)-Biomembranes, 2008. **1778**(10): p. 2210-2216.

113. Kirshenbaum, K., R.N. Zuckermann, and K.A. Dill, *Designing polymers that mimic biomolecules.* Current opinion in structural biology, 1999. **9**(4): p. 530-535.

114. Dohm, M.T., et al., *Mimicking SP-C palmitoylation on a peptoid-based SP-B analogue markedly improves surface activity.* Biochimica et Biophysica Acta (BBA)-Biomembranes, 2010. **1798**(9): p. 1663-1678.

115. Brown, N.J., J. Johansson, and A.E. Barron, *Biomimicry of surfactant protein C.* Accounts of chemical research, 2008. **41**(10): p. 1409.

116. Sanborn, T.J., et al., *Extreme stability of helices formed by water-soluble poly-N-substituted glycines (polypeptoids) with α-chiral side chains.* Biopolymers, 2002. **63**(1): p. 12-20.

117. Mojsoska, B., et al., *Peptoids successfully inhibit the growth of gram negative E. coli causing substantial membrane damage.* Scientific Reports, 2017. **7**: p. 42332.

118. Fowler, S.A. and H.E. Blackwell, *Structure–function relationships in peptoids: recent advances toward deciphering the structural requirements for biological function.* Organic & biomolecular chemistry, 2009. **7**(8): p. 1508-1524.

119. Smith, P.T., M.L. Huang, and K. Kirshenbaum, *Osmoprotective polymer additives attenuate the membrane pore-forming activity of antimicrobial peptoids.* Biopolymers, 2015. **103**(4): p. 227-236.

120. Huang, C.-Y., et al., *Lipitoids—novel cationic lipids for cellular delivery of plasmid DNA in vitro.* Chemistry & biology, 1998. **5**(6): p. 345-354.

121. Lobo, B.A., et al., *Structure/function analysis of peptoid/lipitoid: DNA complexes.* Journal of pharmaceutical sciences, 2003. **92**(9): p. 1905-1918.

122. Turner, J.P., et al., *Modulating amyloid-β aggregation: The effects of peptoid side chain placement and chirality.* Bioorganic & Medicinal Chemistry, 2017. **25**(1): p. 20-26.

123. Picard, F., et al., *31 P NMR first spectral moment study of the partial magnetic orientation of phospholipid membranes.* Biophysical journal, 1999. **77**(2): p. 888-902.

124. Sanders, C.R. and J.P. Schwonek, *Characterization of magnetically orientable bilayers in mixtures of dihexanoylphosphatidylcholine and dimyristoylphosphatidylcholine by solid-state NMR.* Biochemistry, 1992. **31**(37): p. 8898-8905.

125. Vold, R.R. and R.S. Prosser, *Magnetically oriented phospholipid bilayered micelles for structural studies of polypeptides. Does the ideal bicelle exist?* Journal of Magnetic Resonance, Series B, 1996. **113**(3): p. 267-271.

126. van Dam, L., G. Karlsson, and K. Edwards, *Direct observation and characterization of DMPC/DHPC aggregates under conditions relevant for biological solution NMR.* Biochimica et Biophysica Acta (BBA)-Biomembranes, 2004. **1664**(2): p. 241-256.

127. Jiang, Y., H. Wang, and J.T. Kindt, *Atomistic simulations of bicelle mixtures.* Biophysical journal, 2010. **98**(12): p. 2895-2903.

128. Boija, E., et al., *Bilayer disk capillary electrophoresis: a novel method to study drug partitioning into membranes.* Electrophoresis, 2008. **29**(16): p. 3377-3383.

129. Holland, L.A. and A.M. Leigh, *Bilayered phospholipid micelles and capillary electrophoresis: a new additive for electrokinetic chromatography.* Electrophoresis, 2003. **24**(17): p. 2935-2939.

130. Atia, L. and S. Givli, *Biological membranes from the perspective of smart materials – A theoretical study.* International Journal of Solids and Structures, 2012. **49**(18): p. 2617-2624.

131. Smith, A.W., *Lipid–protein interactions in biological membranes: A dynamic perspective.* Biochimica et Biophysica Acta (BBA) - Biomembranes, 2012. **1818**(2): p. 172-177.

132. Venturoli, M., et al., *Mesoscopic models of biological membranes.* Physics Reports, 2006. **437**(1): p. 1-54.

133. Schubert, T. and W. Römer, *How synthetic membrane systems contribute to the understanding of lipid-driven endocytosis.* Biochimica et Biophysica Acta (BBA) - Molecular Cell Research, 2015. **1853**(11, Part B): p. 2992-3005.

Appendices

Appendix A: Scanning Electron Microscopy (SEM) studies

SEM was first used to visualized bicelles and peptoid-functionalized bicelles. The results for bicelle are shown in Figure A.1. However, SEM was not successful in visualizing peptoid-functionalized bicelle due to the charges of peptoids. In order to obtain good images of charged samples, gold coating is usually used which was not applicable in peptoid-functionalized samples. Therefore, TEM was chosen for visualization of bicelles and peptoid- functionalized bicelles.

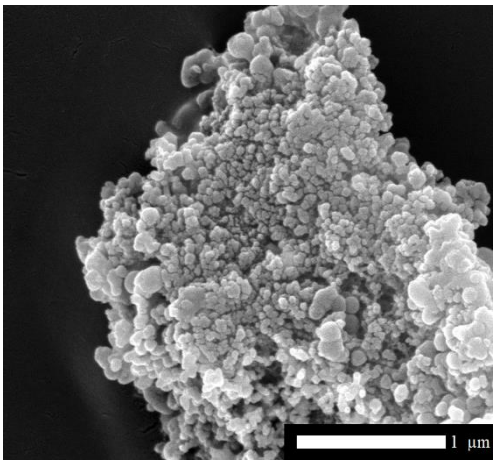

Figure A.1. SEM image of DMPC/DHPC bicelles. Scale bar represents 1 µm.

Appendix B: Using DPPC as the long chain lipid to form bicelles and peptoid-functionalized bicelles

Bicelles and peptoid-functionalized bicelles were also formed using 1,2-dipalmitoyl-sn-glycero-3-phosphocholine (DPPC 16:0 PC) as the long chain lipid which has a longer tail compared to DMPC (14:0 PC). The results show that the addition of peptoid causes a small variation in the size of the bicelles, but does not alter the shape.

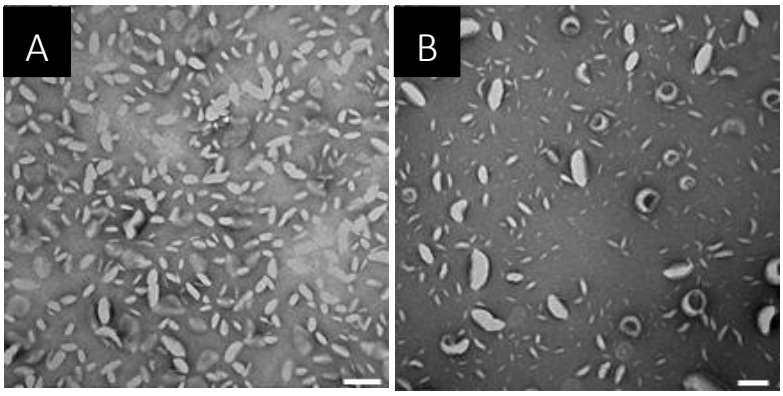

Figure B.1. TEM images of non-functionalized (A) and peptoid-functionalized bicelles using DPPC as long chain lipid. peptoid-DHPC = 0.25 mole% .q=1.5. Scale bar represents 100 nm.